

Neutron Imaging

Gabriele Salvato

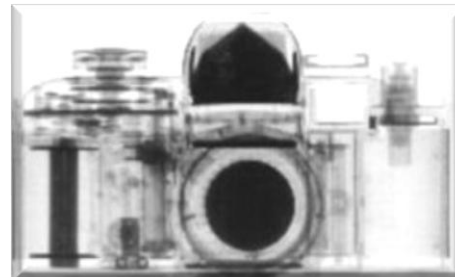
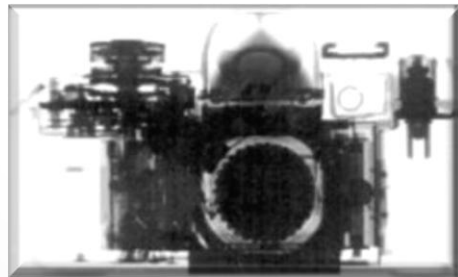
What we will cover

- Attenuation based neutron Imaging
- Energy resolved neutron imaging
- Imaging with polarized neutrons
- Phase contrast neutron imaging

Neutron Imaging

- Is a **non invasive**, **non destructive** technique to obtain images of the inner parts of an object using a neutron beam to illuminate it.
- Resulting images are similar (and they give, in some sense, complementary information) to the ones obtained using X-rays.

X-rays^[*]



Neutrons ^[*]

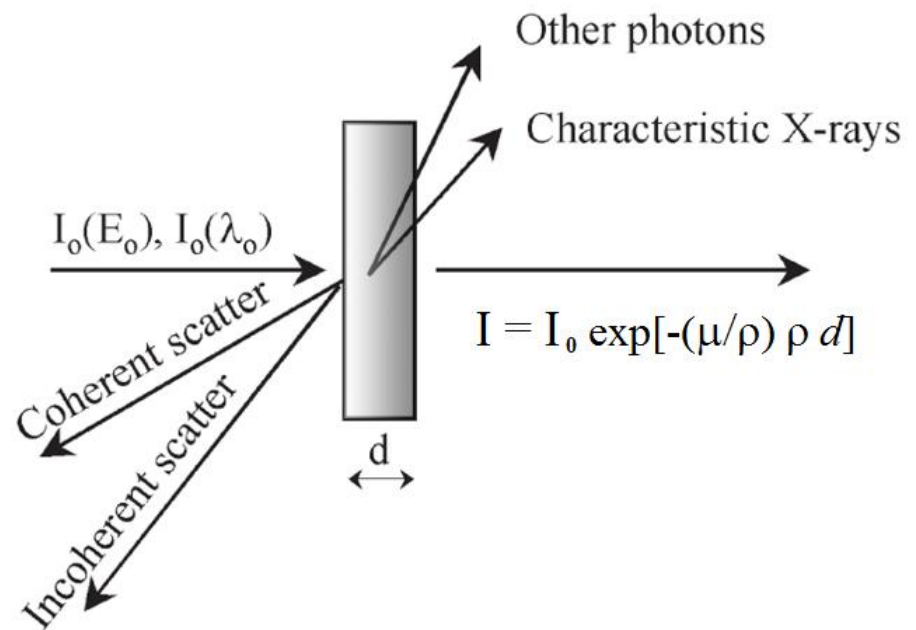
^[*] Lehmann, et al. 2000 - <http://neutra.web.psi.ch/What/index.html>

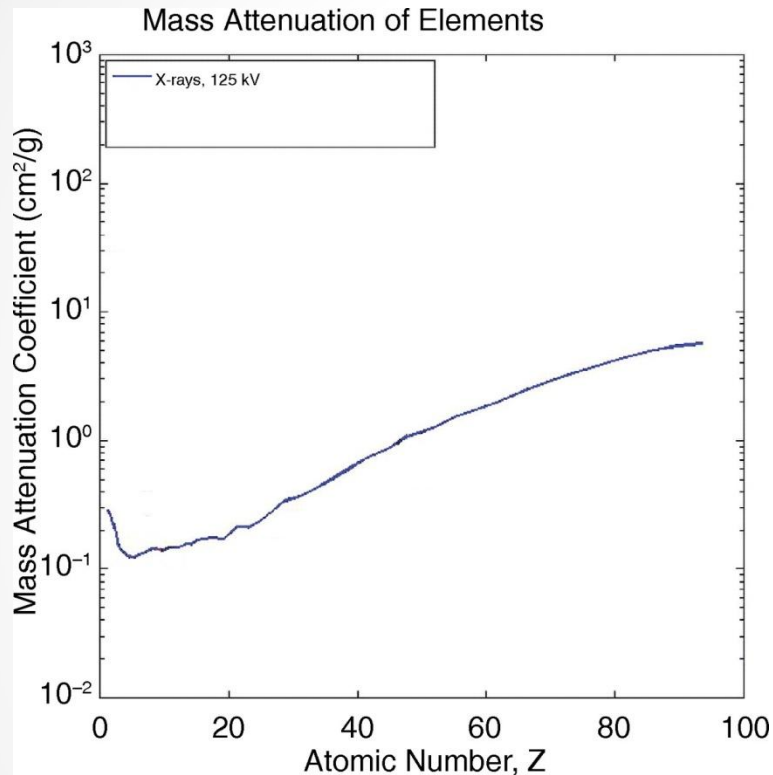
A ***X-ray radiography*** records the attenuation of the *illuminating* beam when it passes through a given object.

The transmission of ***X-rays*** through the matter is described by the ***Lambert-Beer*** law

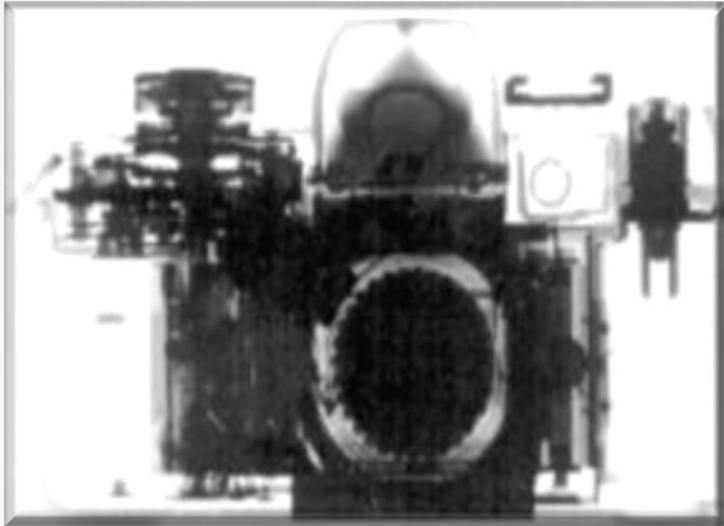
$$I = I_0 e^{-\left[\left(\frac{\mu}{\rho}\right) \rho d\right]}$$

μ / ρ : mass attenuation coefficient [$\text{cm}^2 \text{g}^{-1}$].
 ρ : material density [g cm^{-3}].





The transmitted intensity of **X-rays** is tied to the interaction between X-photons and the ***electronic shells*** of the atoms and it grows, almost linearly, with the atomic number of the elements

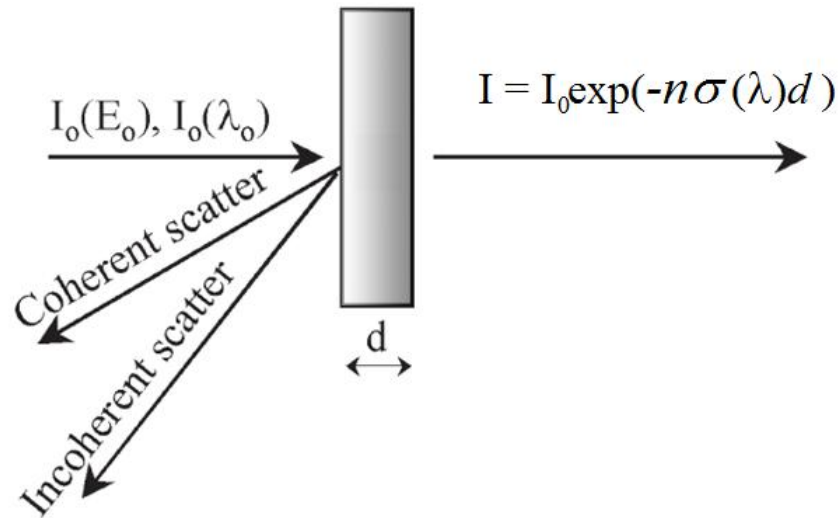


Light elements and ***Hydrogen rich*** materials are almost transparent (invisible) to **X-rays**.

While ***heavy metals*** are almost opaques (impeding to see past).

Materials with similar *Z-number* become almost indistinguishable (they give no image contrast).

The transmission of a **Neutron Beam** is described by the *Lambert-Beer* law too :

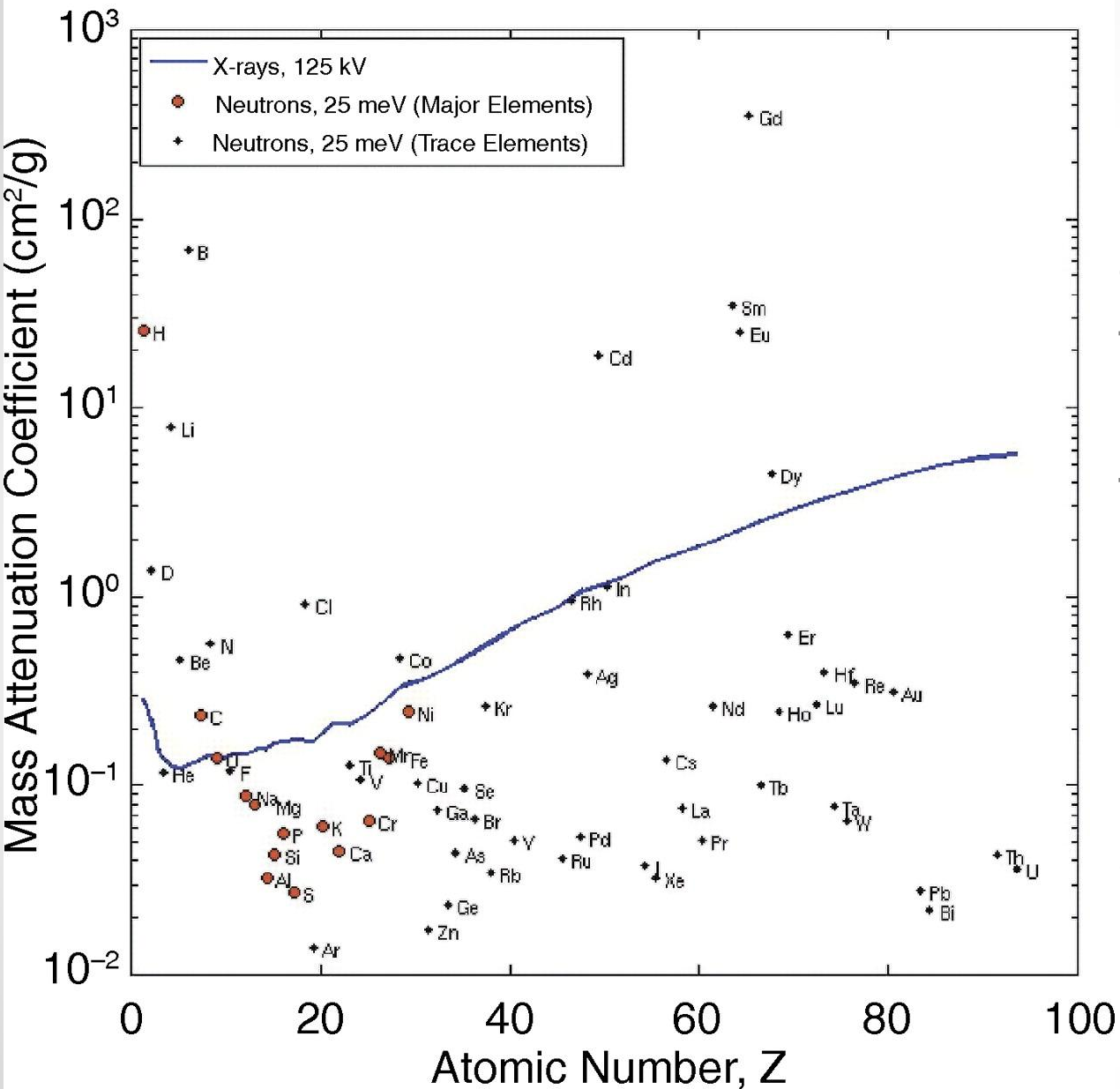


$$I(\lambda) = I_0(\lambda)e^{-n\sigma(\lambda)d}$$

n : scattering center number.

$\sigma(\lambda)$: total cross-section per scattering center.

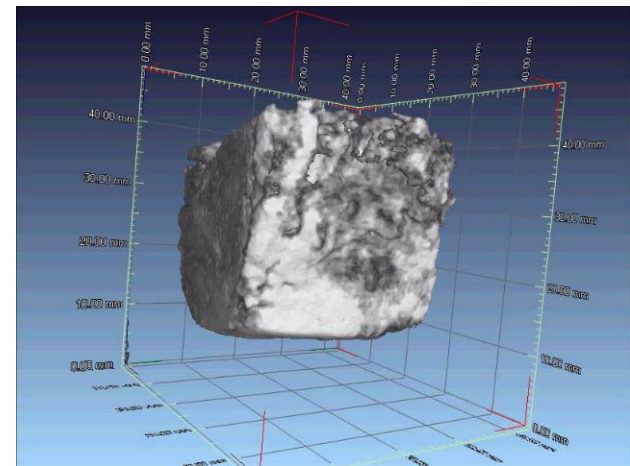
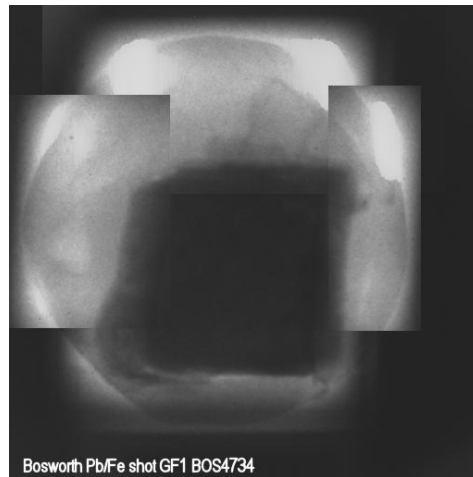
Mass Attenuation of Elements



Because of the charge neutrality of neutrons the transmitted intensity is **NOT** tied to the Z number but instead it is *randomly distributed* among different materials.

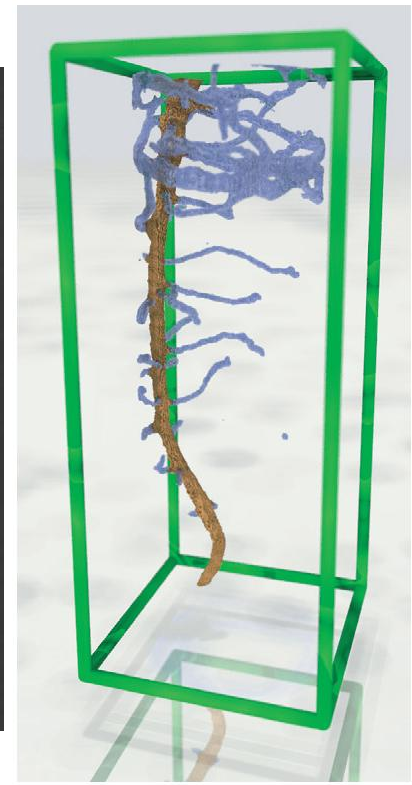
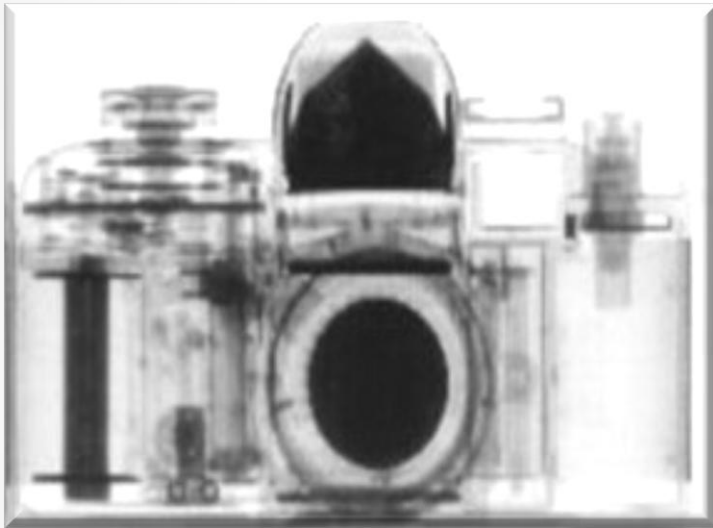
Heavy metals (*Pb*, *Fe*), almost opaque to *X-rays*, can be imaged with good contrast with neutrons.

Lead's cannonball from the *Bosworth Field* (1485) battle. (*Wars of the Roses*)



E. Godfrey, W. Kockelmann, G. Salvato, D. Tresoldi "Non-invasive Neutron Techniques: implications for analysis of battlefield artefacts" (2010)

Light atoms (H , Li , B), almost transparent to X -rays, give a good contrast when imaged with neutrons.



12-d-old chickpea plant grown in a cylinder filled with a sandy soil

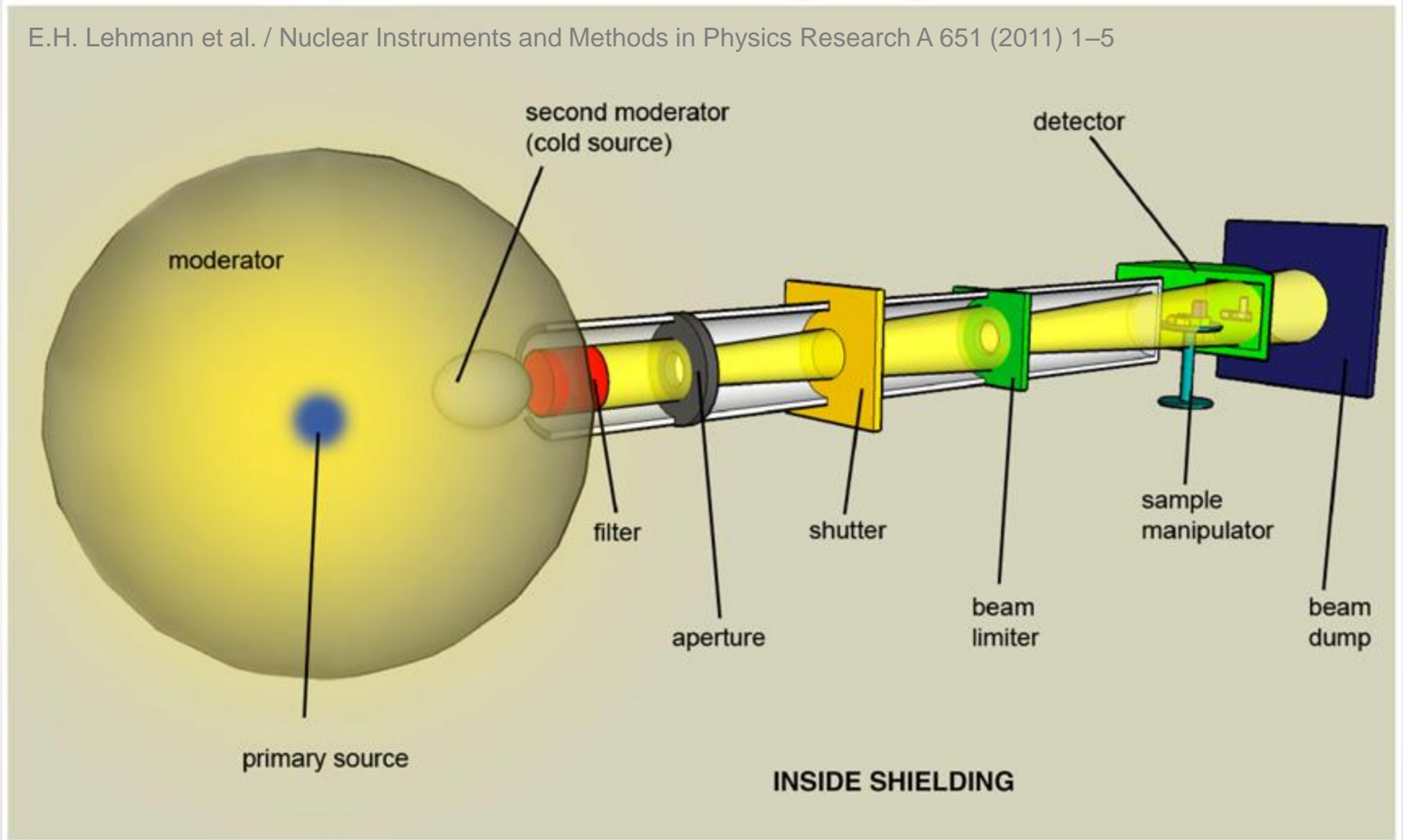
Ahmad B. Moradi et al. *New Phytologist* 192, 653–663 (2011)

Neutrons give different image contrast between materials with similar Z numbers and also *between different isotopes* of the same substance.

Isotope	absorption cross section for 1.8Å neutrons	Isotope	absorption cross section for 1.8Å neutrons
^1H	0.3326	^2H	0.000519
^6Li	940	^7Li	0.0454
^3He	5333	^4He	0.000...
^{10}B	3835	^{11}B	0.0055
^{157}Gd	259000	^{158}Gd	2.2

How Neutron Imaging is done ?

E.H. Lehmann et al. / Nuclear Instruments and Methods in Physics Research A 651 (2011) 1–5



Neutron Sources (for research)

Reactor Based

Accelerator
Based

Very High
Flux

Pulsed

Continuous

Medium to High
intensity

Not every neutron facility provides neutron imaging beamlines. Here are listed the most successful but more are coming ,e.g. *IMAT* at ISIS (UK), *ESS* in Lund (Sweden).

Table 2

Neutron imaging facilities with state-of-the-art properties and conditions (without claim for completeness); given parameters are raw values that can be varied only by changing beam conditions.

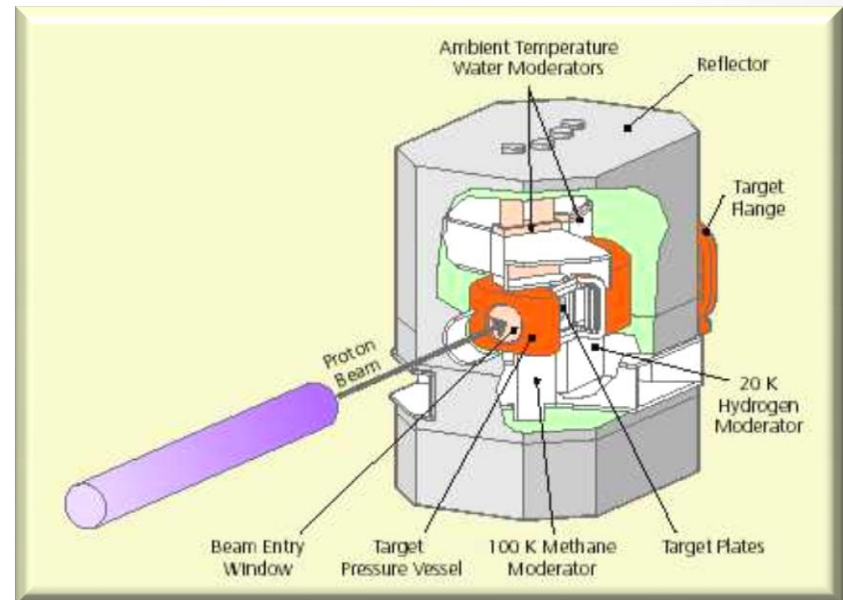
Country	Location	Institution	Facility	Neutron source	Thermal/cold flux ($\text{cm}^{-2} \text{s}^{-1}$)	L/D ratio	Field of view
Austria	Vienna	Atominstitut	Imaging beam line	TRIGA Mark-II, 250 kW	1.00E+05	125	90 mm diam.
Brazil	Sao Paulo	IPEN	Imaging beam line	IEA-R1M 5 MW	1.00E+06	110	25 cm diam.
Germany	Garching	TU Munich	ANTARES	FRM-II 25 MW	9.40E+07	400	32 cm diam.
Germany	Garching	TU Munich	NECTAR	FRM-II 25 MW	3.00E+07	150	20 cm diam.
Germany	Berlin	HZB	CONRAD	BER-II 10 MW	6.00E+06	500	10 cm × 10 cm
Hungary	Budapest	KFKI	Imaging beam line	WRS-M 10 MW	6.00E+05	100	25 cm diam.
Japan	Osaka	Kyoto University	Imaging beam line	MTR 5 MW	1.20E+06	100	16 cm diam.
Japan	Tokai	JAEA	Imaging beam line	JRRM-3M 20 MW MTR	2.60E+08	125	25 cm × 30 cm
Korea	Daejon	KAERI	Imaging beam line	HANARO 30 MW	1.00E+07	190	25 cm × 30 cm
Switzerland	Villigen	PSI	NEUTRA	SINQ spallation source	5.00E+06	550	40 cm diam.
Switzerland	Villigen	PSI	ICON	SINQ spallation source	1.00E+07	350	15 cm diam.
USA	Pennsylvania State University	University	Imaging beam line	TRIGA 2 MW	2.00E+06	100	23 cm diam.
USA	Gaithersburg	NIST	CNR	NBSR 20 MW	2.00E+07	500	25 cm diam.
USA	Sacramento	McClellan RC	Imaging beam line	TRIGA 2 MW	2.00E+07	100	23 cm diam.
South Africa	Pelindaba	NECSA	SANRAD	SAFARI-1 20 MW	1.60E+06	150	36 cm diam.

E.H. Lehmann et al. / Nuclear Instruments and Methods in Physics Research A 651 (2011) 1–5

Neutron moderation

The neutron energy spectrum is inadequate for the material structure investigations and must be reduced into a **wavelength range of $\sim 0.5\text{-}10\text{\AA}$**

To reduce the neutron energies, they are sent to a “*moderator*” that slows the incoming neutron beam.



D.Findlay “Introduction to ISIS accelerator and target” (2006)

Gamma and Neutron Filters

Gamma and neutron filters are required to filter out the gamma rays and fast neutrons from the beam.

The presence of gamma-ray in the imaging beam can cause *foggy* images.

Both, gammas and fast neutrons, can damage electronic devices.

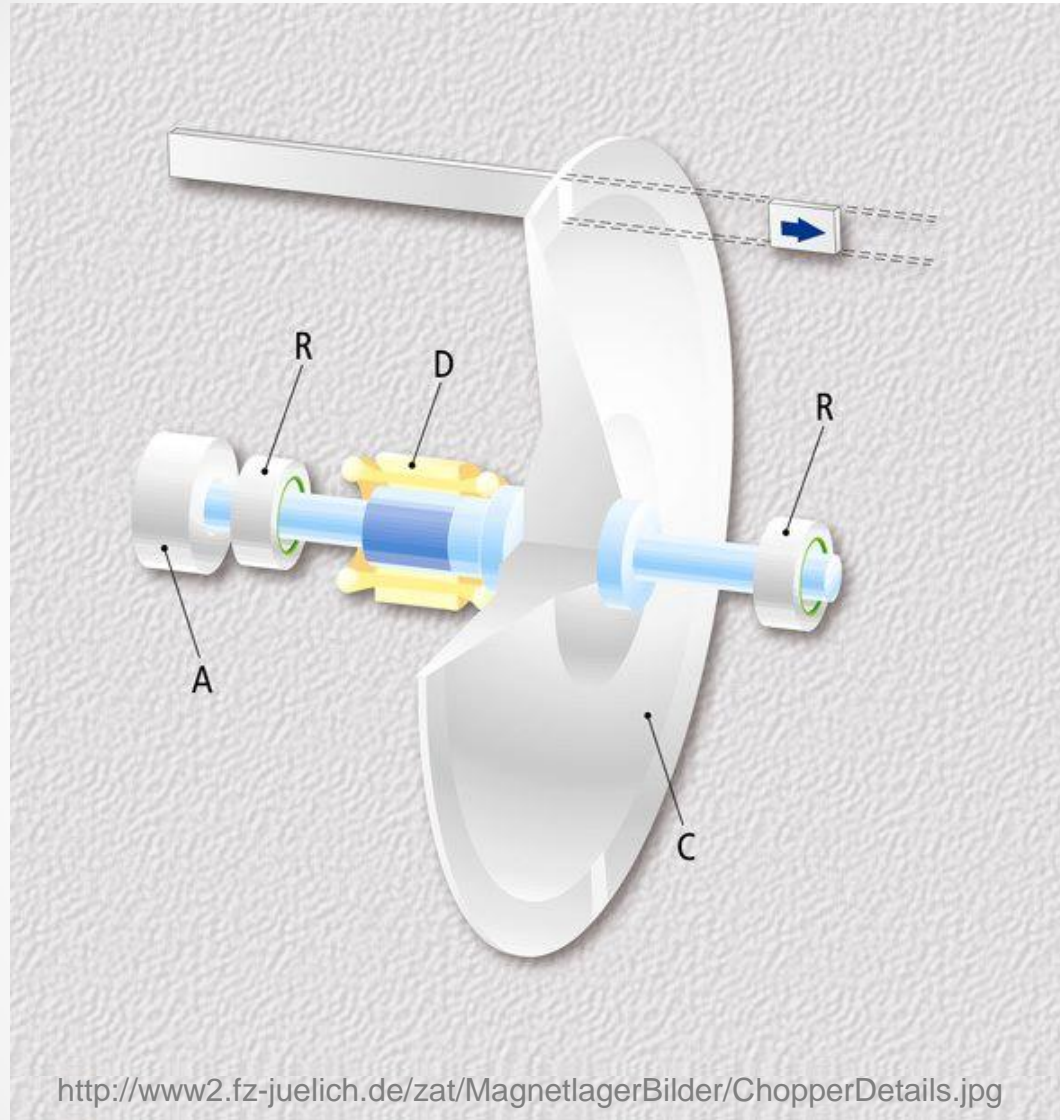
At pulsed spallation sources, filters are realized by choppers synchronized with the spallation pulse. They are called...

T₀ Choppers

Fast neutrons arrive at the chopper position immediately after the proton pulse strikes the target.

The T₀ chopper must be able to place a large mass of high-cross-section material in the neutron beam during the brief time the fast neutrons are present.

T₀ choppers must rotate rapidly so to leave the beam unblocked when neutrons of the desired wavelengths are traveling through the chopper position.



<http://www2.fz-juelich.de/zat/MagnetlagerBilder/ChopperDetails.jpg>

T₀ Choppers

IMAT

2 CAMERAS:

Medium resolution screen (200x200mm)

High resolution screen (30x30mm)

5 JAW sets with 200x200 mm apertures
will shape the beam

A PIN HOLE SELECTOR at 46 Metres will project
varied enlarging circular beams up to 200mm
diameter onto the S1 sample.

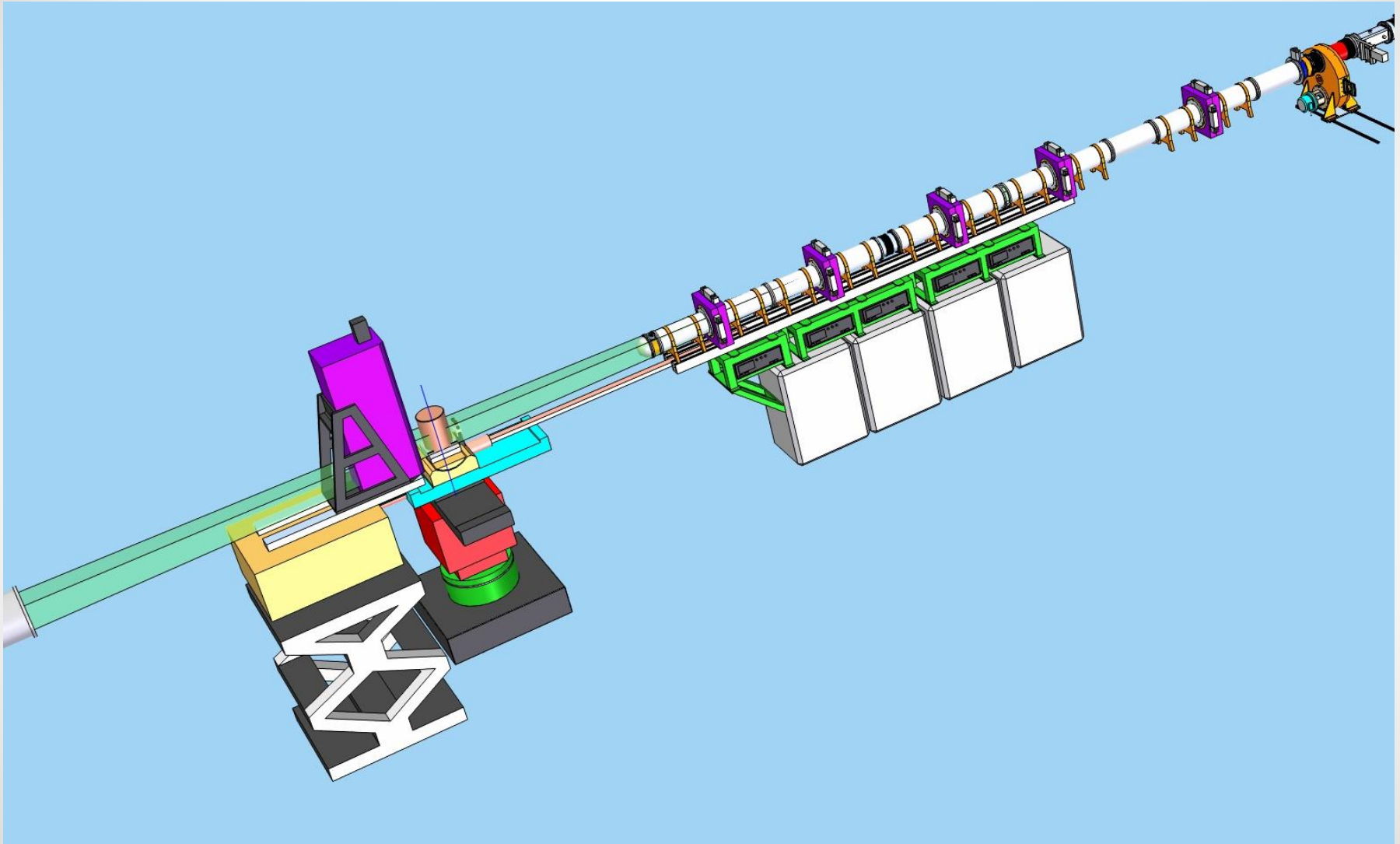
Sample S1

95 mm square neutron beam

T₀ Chopper set

Source repetition	10 Hz
Moderator	Liquid H ₂ / solid CH ₄ coupled
Primary neutron guide	m=3 straight, square, 95x95 mm
Single frame bandwidth	0.6 - 6.5 Å
Double frame bandwidth	2 - 14 Å
Flight path to sample	56 m

IMAT - imaging beamline components



How to detect Neutrons ?

Because of their charge neutrality, neutrons are difficult to detect. Instead, we are able in detecting charged particles.

A nuclear reaction is necessary to convert incoming neutrons into charged particles.

Depending on the employed image sensor further conversions can be necessary. If the image formation sensor is a digital camera the charged particles must be converted into photons.

A number of different reactions can be used to convert neutrons into charged particles. Main reactions employed: [1]



$$\sigma = 28000 \text{ b}$$



$$\sigma = 520 \text{ b}$$

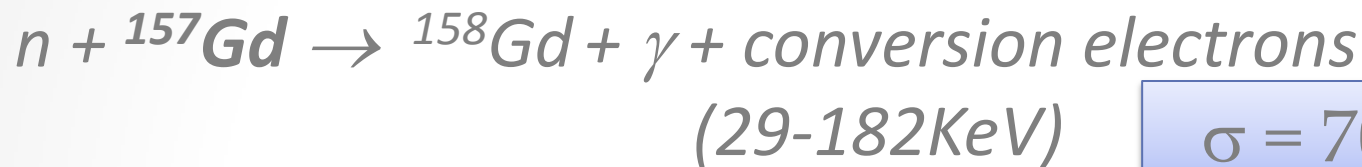


$$\sigma = 2100 \text{ b}$$

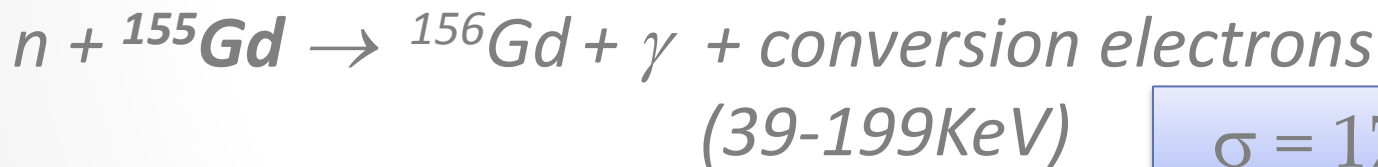
$$\sigma @ 1\text{\AA}$$

[1] C.W.E. van Eijk Nucl. Instr. And Meth. A 477 383 (2002)

Other reactions employed: [1]

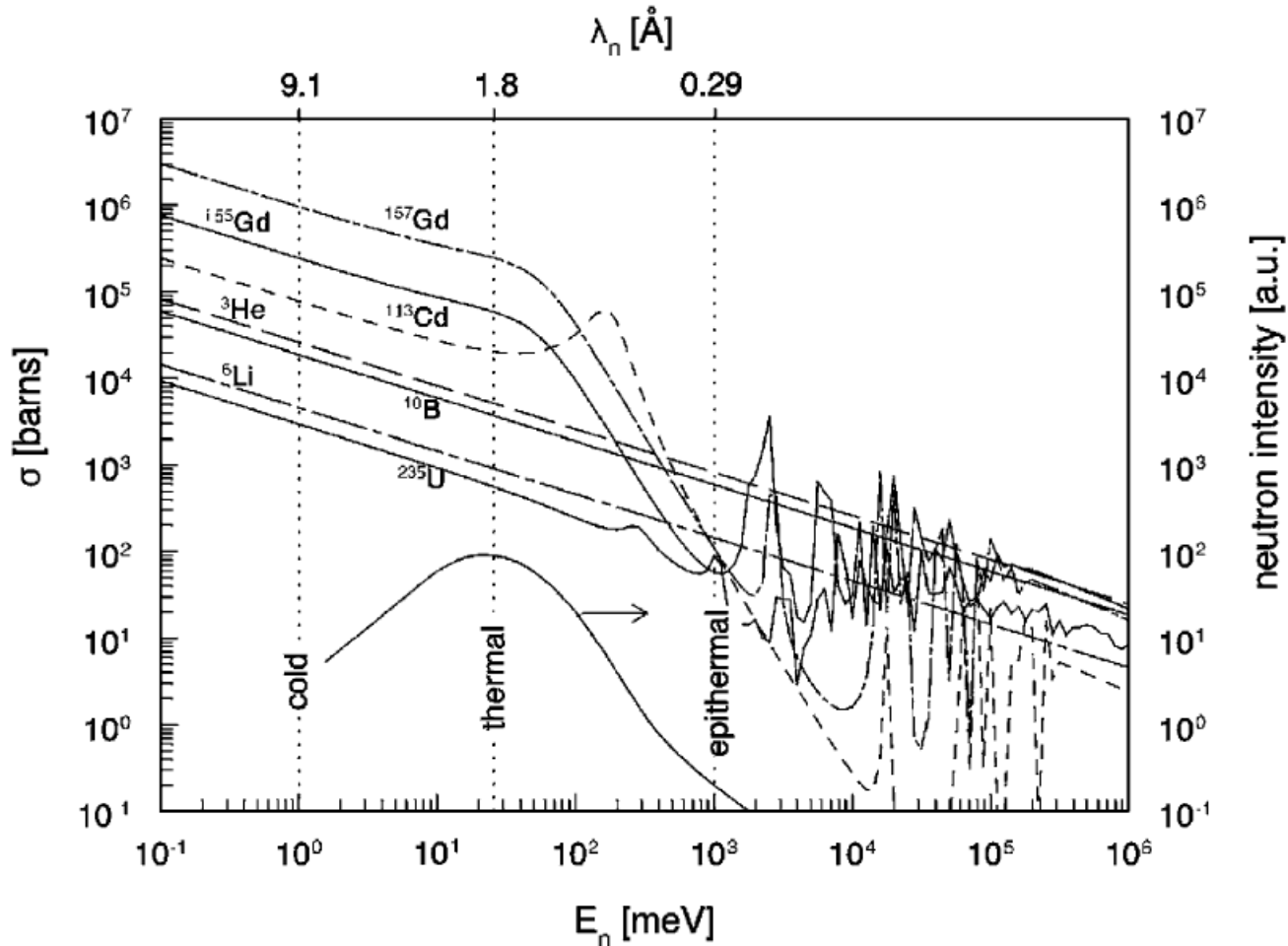


$$\sigma = 70000 \text{ b}$$



$$\sigma = 17000 \text{ b}$$

$$\sigma @ 1\text{\AA}$$

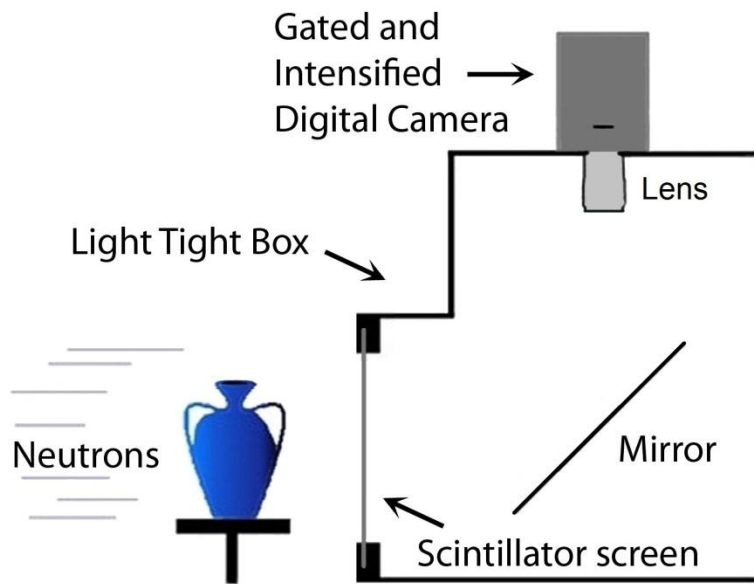


Neutron capture cross-sections of some isotopes important for neutron detectors as a function of neutron energy. The lowest curve shows a typical moderated neutron spectrum of a nuclear reactor (right y-axis) [1].

[1] C.W.E. van Eijk Nucl. Instr. And Meth. A **477** 383 (2002)

Digital Camera based Imaging Systems

With the advent of digital imaging systems (and brighter neutron sources as well) neutron imaging has seen a very fast development.



Neutrons transmitted through the sample strike a scintillator screen which converts the incoming neutrons into photons detected, through a mirror, by a digital camera.

The most used scintillator screens are made by a mix of finely grounded ${}^6\text{LiF}$ and ***ZnS:Ag*** or ***ZnS:Cu***.

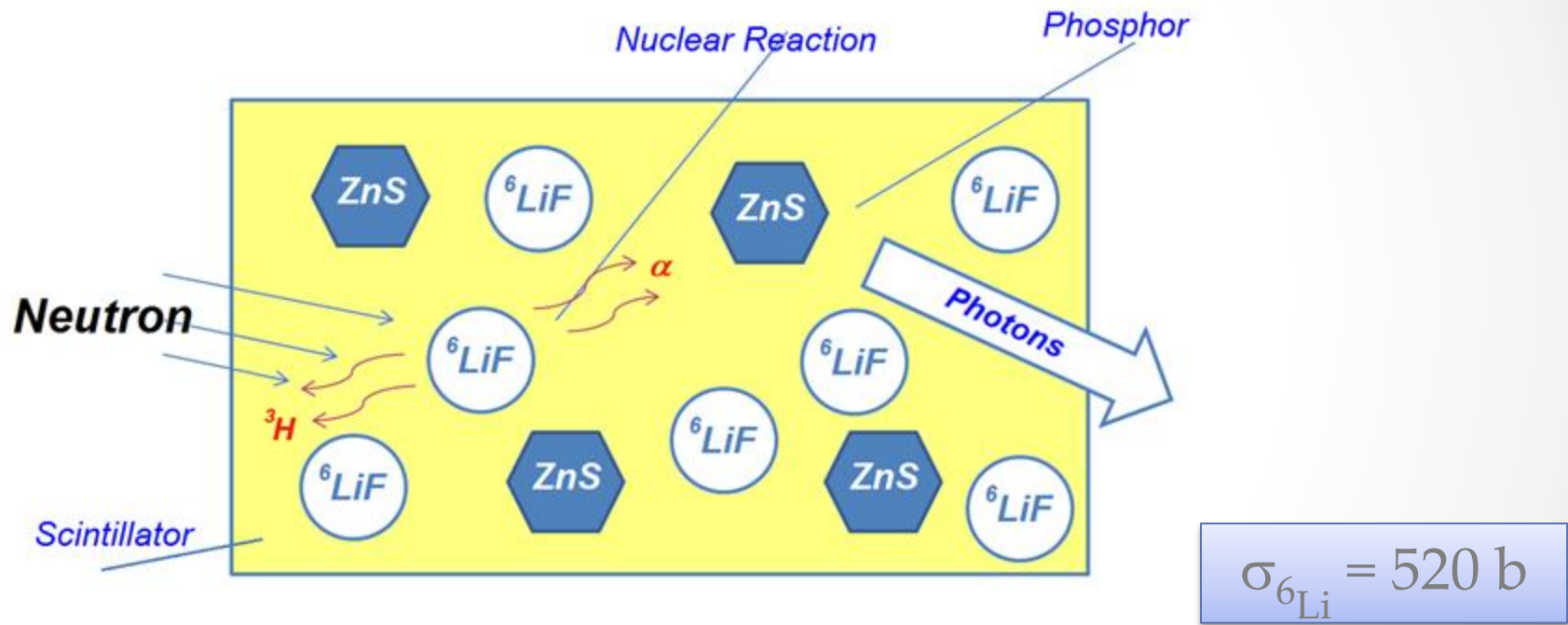
The ${}^6\text{LiF}$ and ***ZnS*** powders are mixed with an organic binder and deposited on a thin ***Al*** foil.

The ***Al*** foil is almost transparent to neutrons but it stops the light from the outside.

When a ${}^6\text{Li}$ atom interacts with a neutron it emits a *Triton* and an α particle. The respective ranges are about $130\mu\text{m}$ and $5\mu\text{m}$ [1].

[1] T.K. McKnight Master Thesis - Dep. Of Physics and Astronomy – Brigham Young University (2005)

The particles interact with the **ZnS** phosphor producing about **160.000 photons per neutron**^[1].



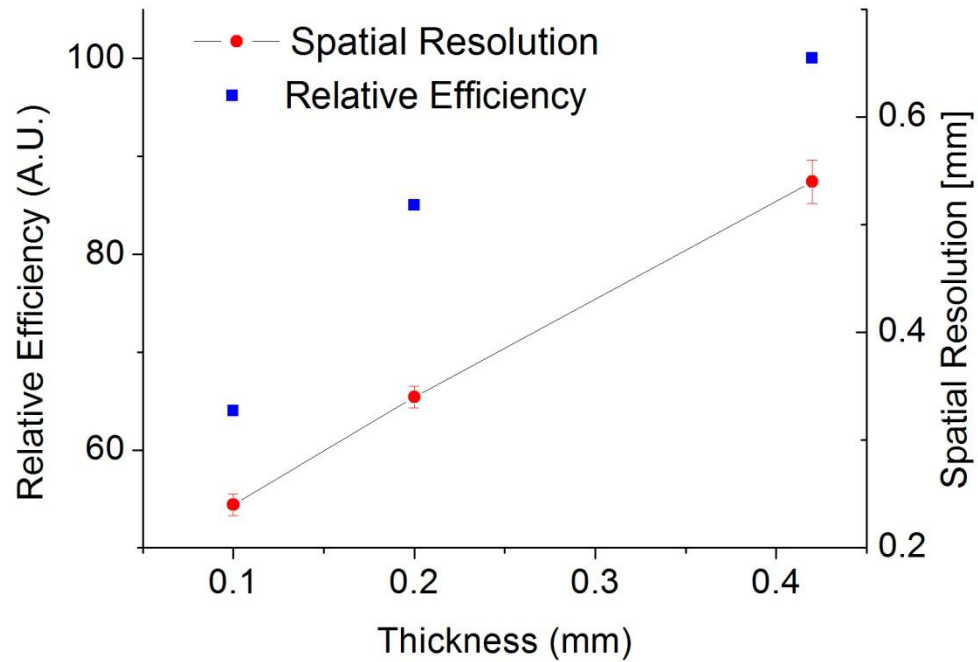
[1] C.W.E. van Eijk Nucl. Instr. And Meth. A **477** 383 (2002)

The conversion efficiency of the ${}^6\text{LiF/ZnS}$ scintillators grows with their thickness **BUT** ...

- ➔ since the material *is opaque at its own radiation* the thickness cannot be greater than 0.4 ~ 0.5mm.
- ➔ Because of the range of the secondary particles in the material, the light can be produced in a position different from the neutron interaction limiting the *spatial resolution* that can be reached. The spatial resolution decreases as their thickness increases.

${}^6\text{LiF/ZnS:Ag}$ scintillator

S. Baechler et al. Nucl. Instr. and Meth. A **491** 481-491 (2002)



The ultimate limit to the spatial resolution is given by the range of the particles generated by a neutron capture event.

Thinner scintillators improve the spatial resolution but decrease the efficiency. This implies much longer exposure times. Other converter materials with higher cross-section for slow neutrons are necessary.

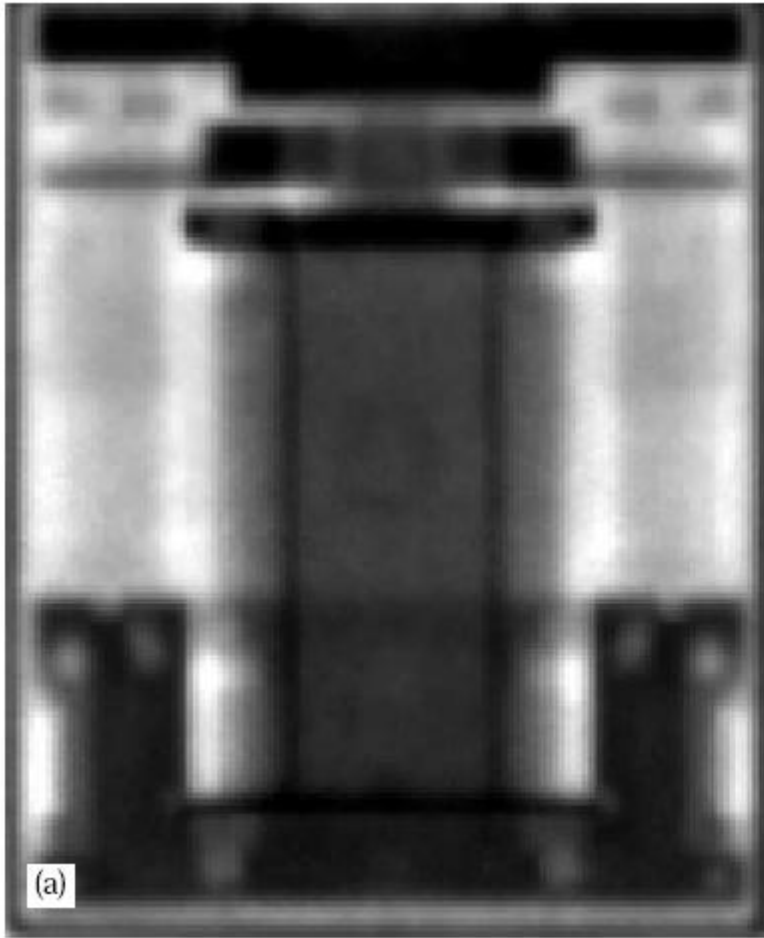
Very recently, the research group led by N. Kardjilov produced a new scintillator screen based on $Gd_2O_2S(Tb)$ able to absorb 90% of the neutrons with a layer thickness of only $10\mu\text{m}$ [1].

Because of lower conversion efficiency of *gadox* in comparison to ${}^6\text{LiFZnS(Ag)}$ (by roughly two orders of magnitude) and being highly sensitive to gammas, a large number of “white-spots” were observed.

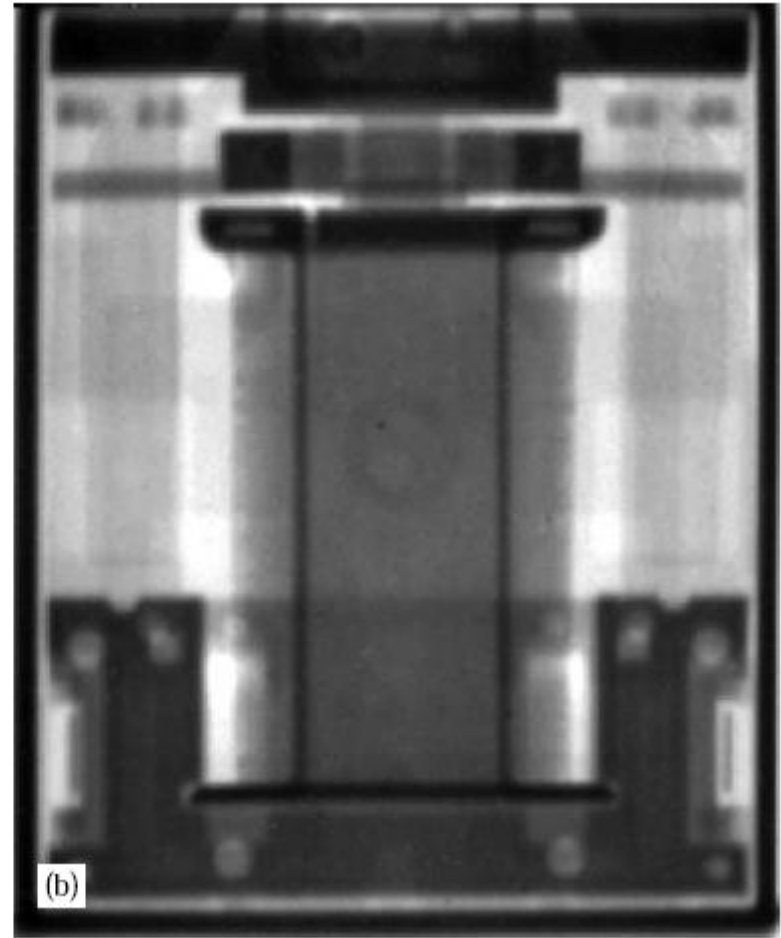
To measure one high quality image with it is therefore necessary to record multiple long-exposure images and to apply erosion/median filters to reduce the levels of noise^[1].

Their detector allowed to obtain high-quality neutron imaging with a spatial resolution of $25\mu\text{m}$.

[1] N. Kardjilov et al. Nucl. Instr. and Meth. A 651 95-99 (2011)



(a) 0.40-mm-thick converter



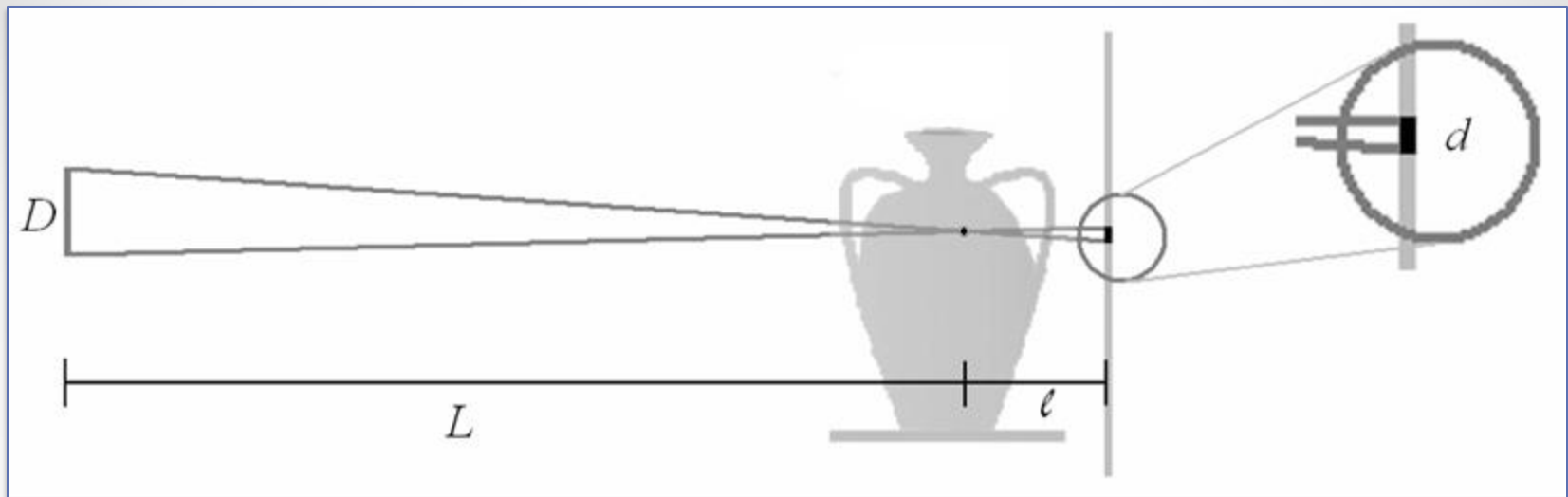
(b) 0.10-mm-thick converter.

S. Baechler et al. Nucl. Instr. and Meth. A **491** 481-491 (2002)

The spatial resolution of a neutron imaging system is tied to many aspects of the experimental setup and not only to the scintillator characteristics.

Among them there are the *number of pixels* of the image sensor, the *field of view dimensions* and the employed *optics*.

Moreover, *the neutron source cannot be considered as a point-like one*. It has a cross-sectional dimension that must be taken into account.



D = neutron source dimension

L = source-sample distance

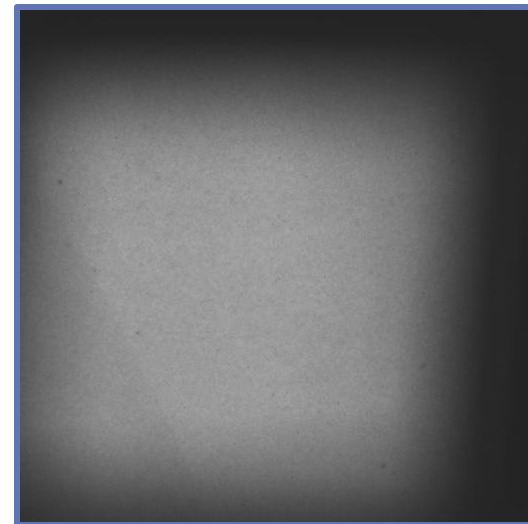
ℓ = source-scintillator distance

$$d = \ell \frac{D}{L} = \frac{\ell}{L/D}$$

Beam collimation values (L/D) greater than 1000 could be found in dedicated neutron imaging beamlines

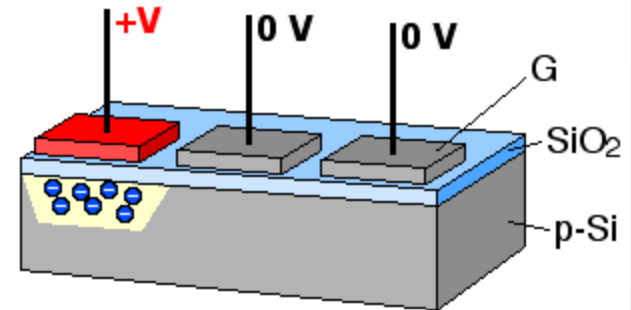
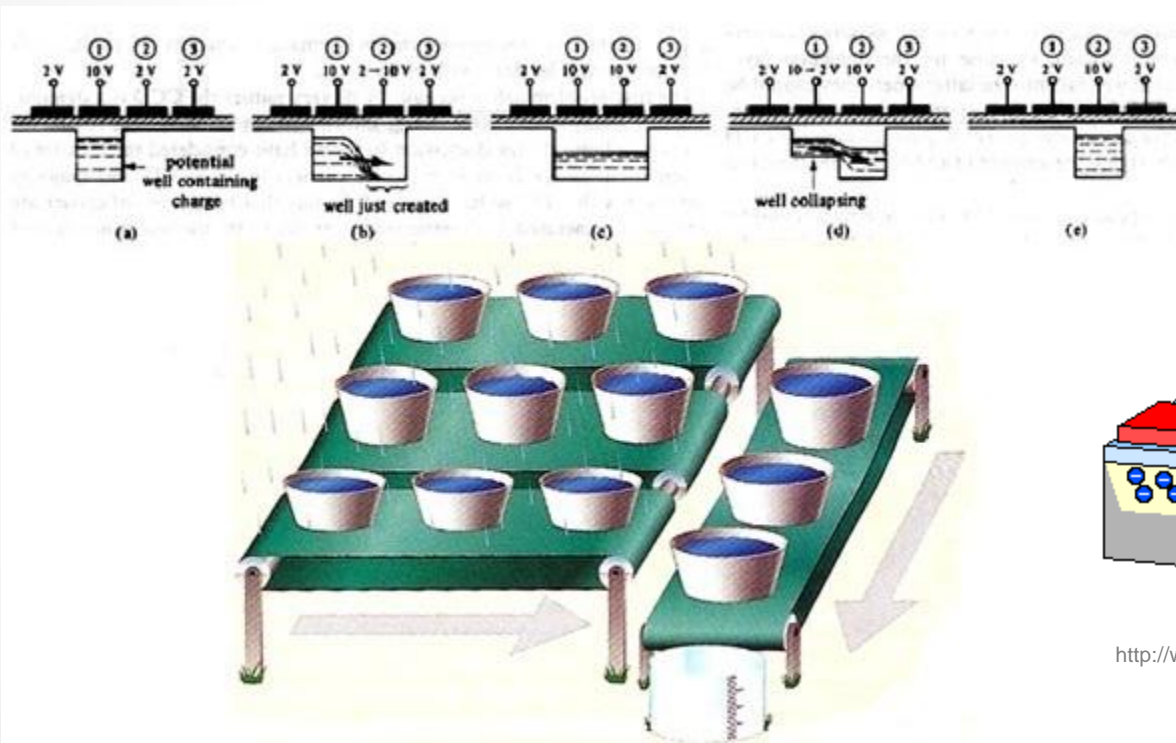
Relevant Beam parameters:

- Beam spectrum ($\sim 1 - 7 \text{ \AA}$);
- Beam Intensity ($> 10^7 \sim 10^8 \text{ n} \cdot \text{s}^{-1} \cdot \text{cm}^{-2}$);
- Beam collimation value ($L/D > 500$);
- Beam dimensions ($L \times W > 20 \times 20 \text{ cm}^2$);
- Beam profile.



CCD based image sensors

Charged Coupled Devices (CCD) are image sensors developed mainly for consumer cameras.



<http://weareallinthegutter.wordpress.com/2010/09/>

<http://www.science.ca/images/scientists/s-boyle-infographic.jpg>

CCDs are *very linear devices*: the number of collected electrons in a pixel is proportional to the number of incident photons.

Smaller *pixel size* will give better spatial resolution but will limit the amount of charge that can be stored in a pixel (*full well capacity*) before saturation.

This, in turn, will limit the *dynamic range* of the device.

However, bigger pixel size increases the dark current and the device must be cooled at lower temperature.

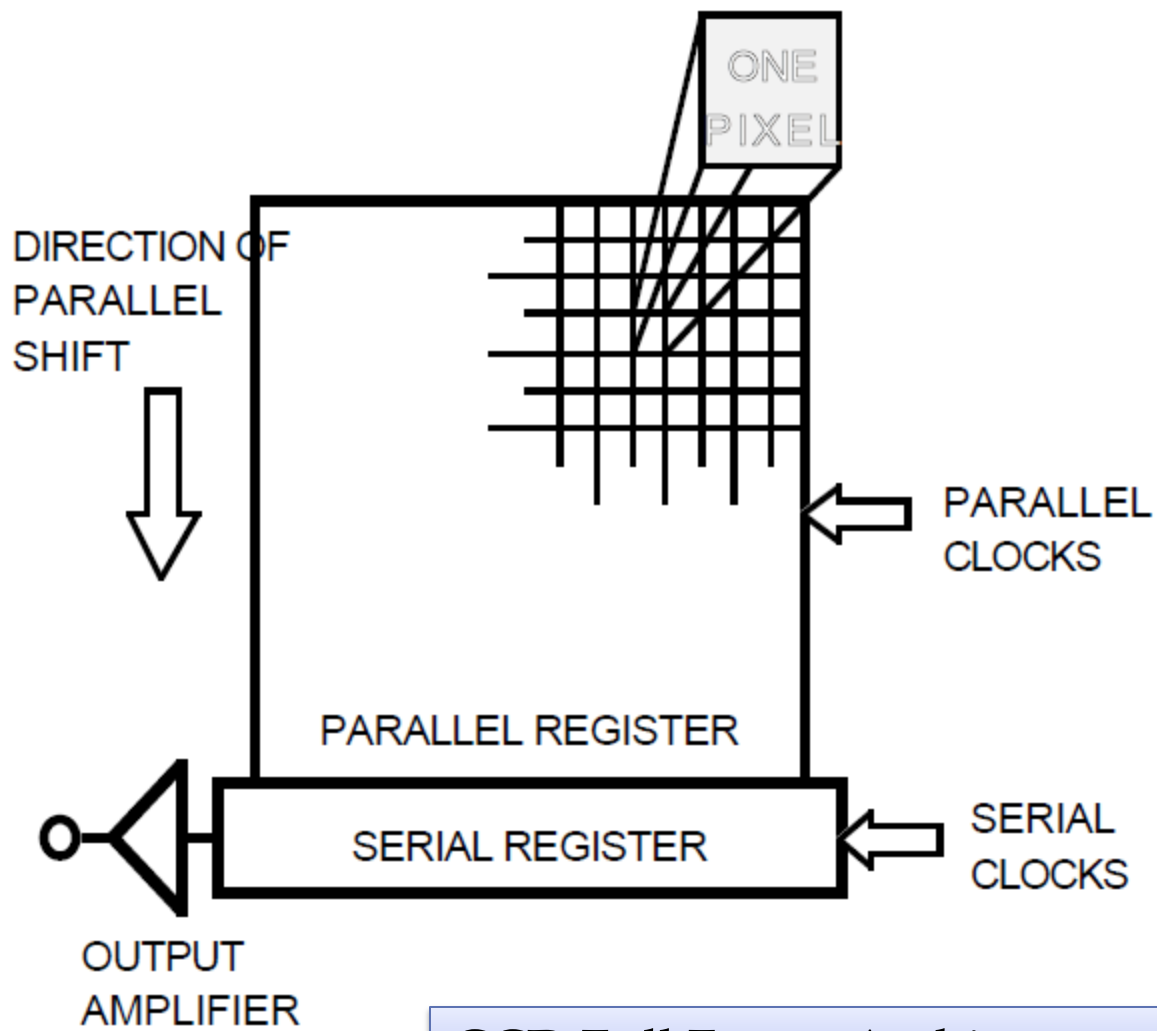
Most CCD cameras for research are cooled either by *Peltier cells* or by a circulating liquid.

Since the *A/D* conversion is made by a single converter, there are no big differences between pixels. However small different sensitivity can be present in each pixel. These differences can be reduced by appropriate image post-processing.

The ***number of bits*** of the *A/D converter* is also important to define the dynamic range of the images.

Apart from the thermal noise, the main source of noise in the *CCD*'s is the ***readout noise***. The faster is the image readout, the bigger is the readout noise contribution. For this reason the readout of research cameras is deliberately very slow.

Quantum efficiency (QE), the *light-to-charge* efficiency conversion, is another fundamental parameter of *CCD*'s. This must be maximized at the emission wavelength of the scintillator.

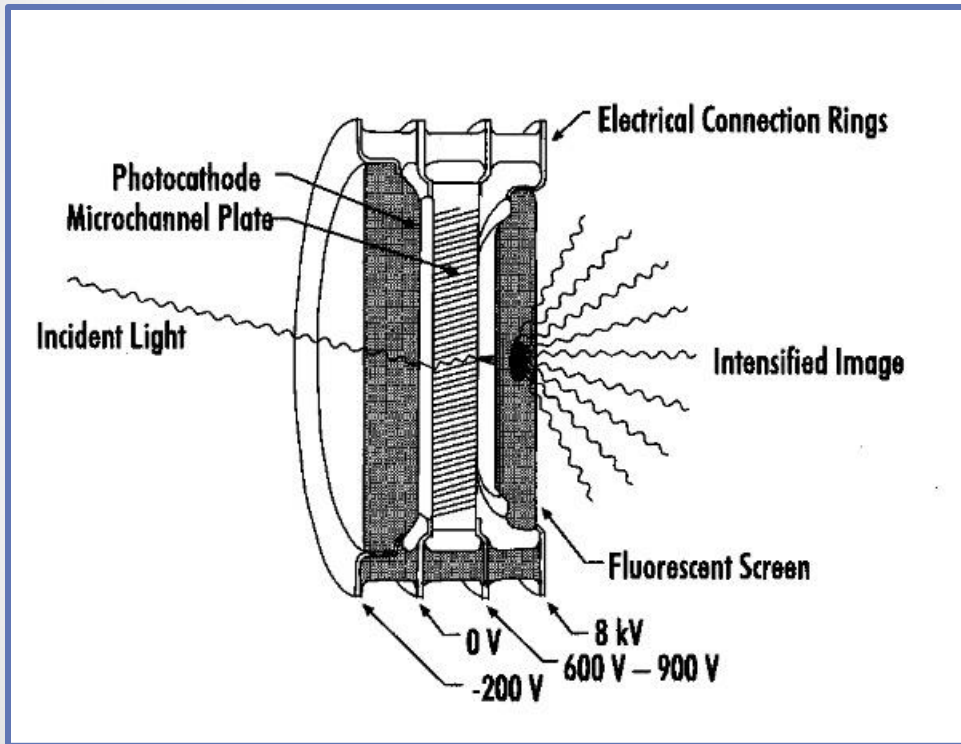


CCD Full Frame Architecture

The incoming light continues to fall onto the sensor even during the readout causing the smearing of the image.

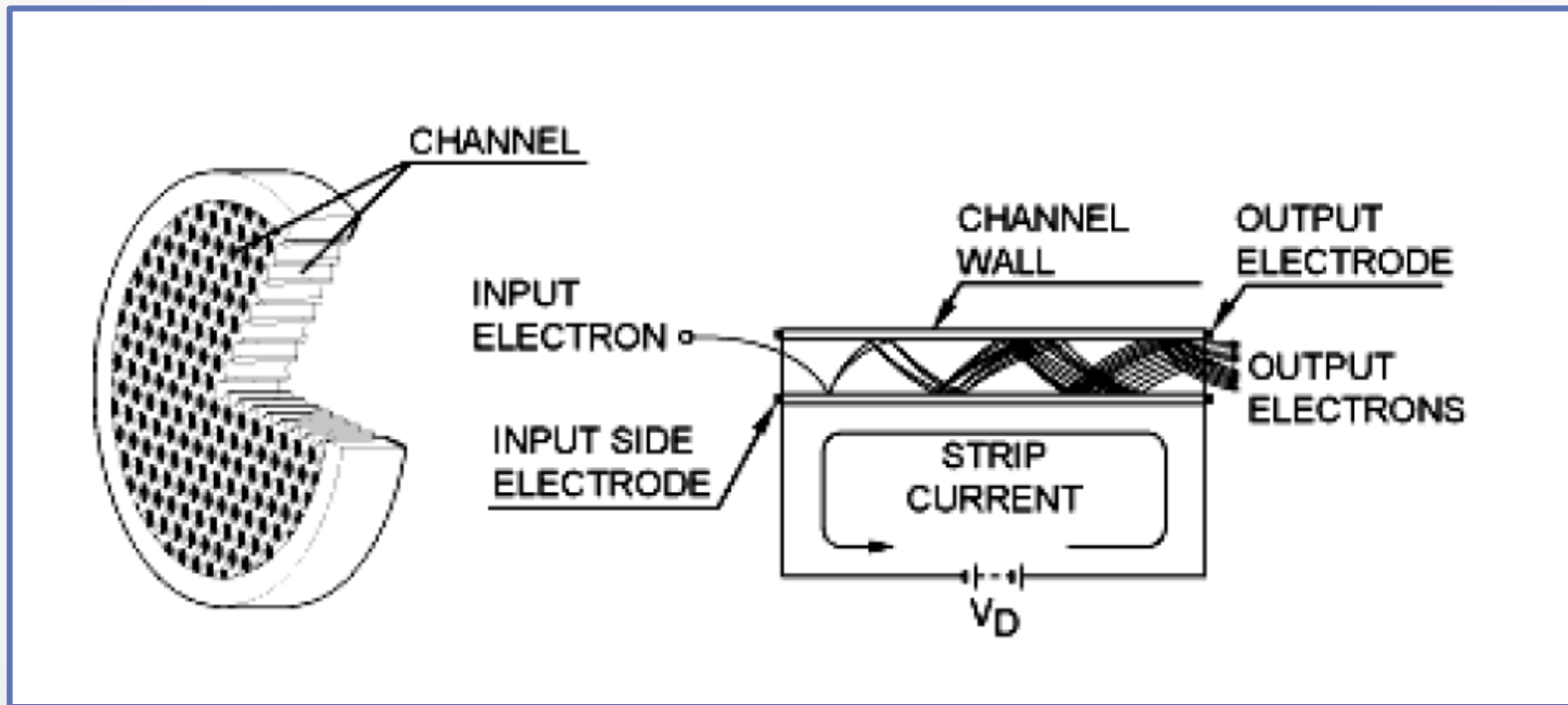
This can be avoided by using a *shutter*.

The *shutter* can be realized by interposing between the lens and the **CCD** sensor a **Gated Image Intensifier**.

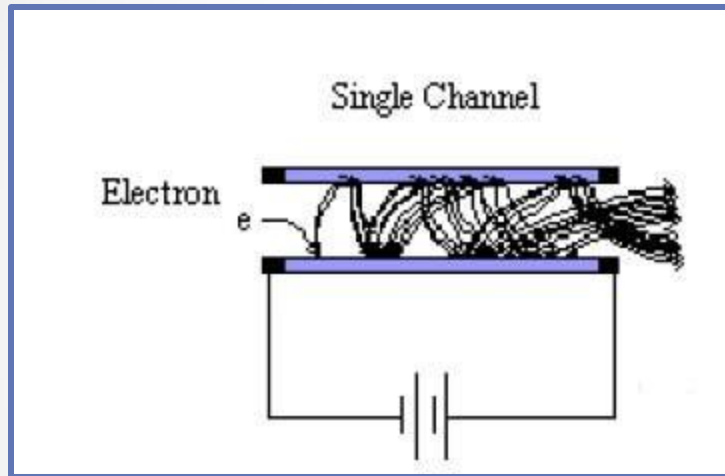


The photons reaching the *microchannel plate* generate charged particles that are accelerated by an electric field and made to collide with a fluorescent screen.

The *micro channel plate* is a thin disk (<1 mm thick) of honeycombed glass, and each of the honeycomb channels ($\sim 6\text{-}10\mu\text{m}$) has a resistive coating.



The micro channel plate has a high potential across it (500 to 1000 V). The photoelectron will cascade down the channel producing secondary electrons; the resultant amplification can be up to 10^4 .

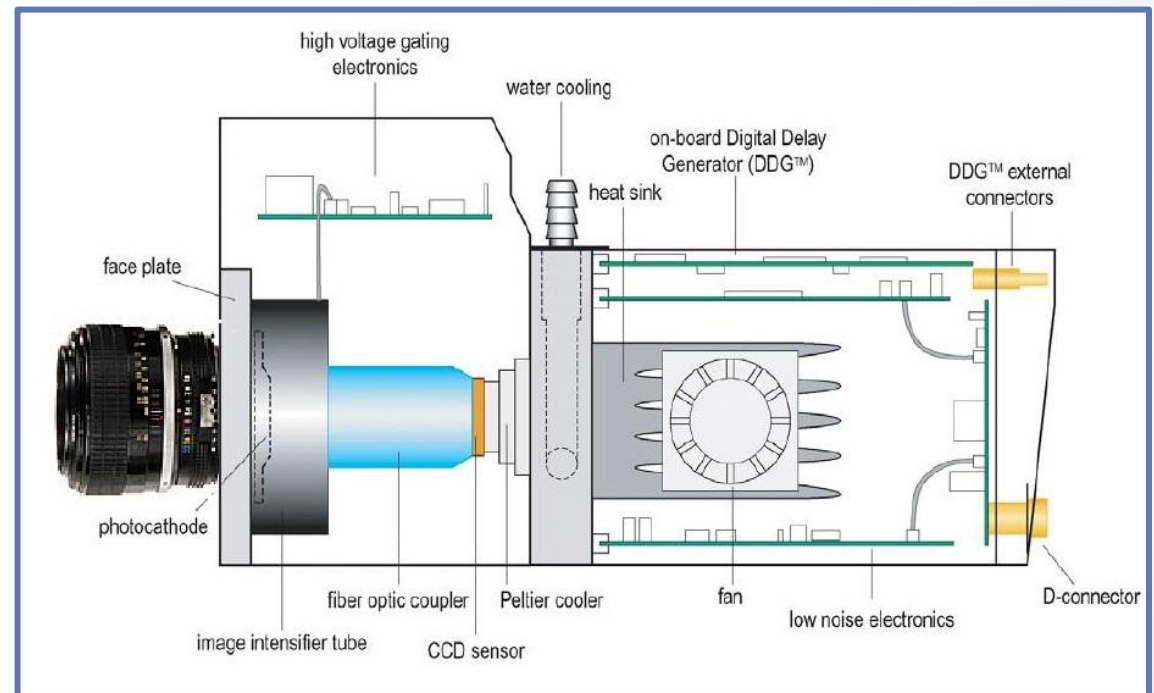


Varying the voltage across the channel plate it is possible to ***control the gain.***

Changing the voltage across the microchannel plate it is possible to ***completely stop*** the light that reaches the CCD sensor (the on/off ratio is $\sim 1:10^8$).

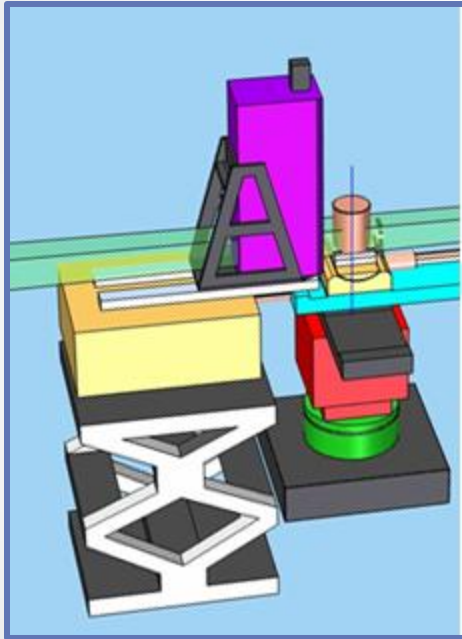
The image shows a schematic view of an *Andor iStar* camera.

Very bright lenses (high numerical aperture) must be used in order to reduce the required total exposure time.



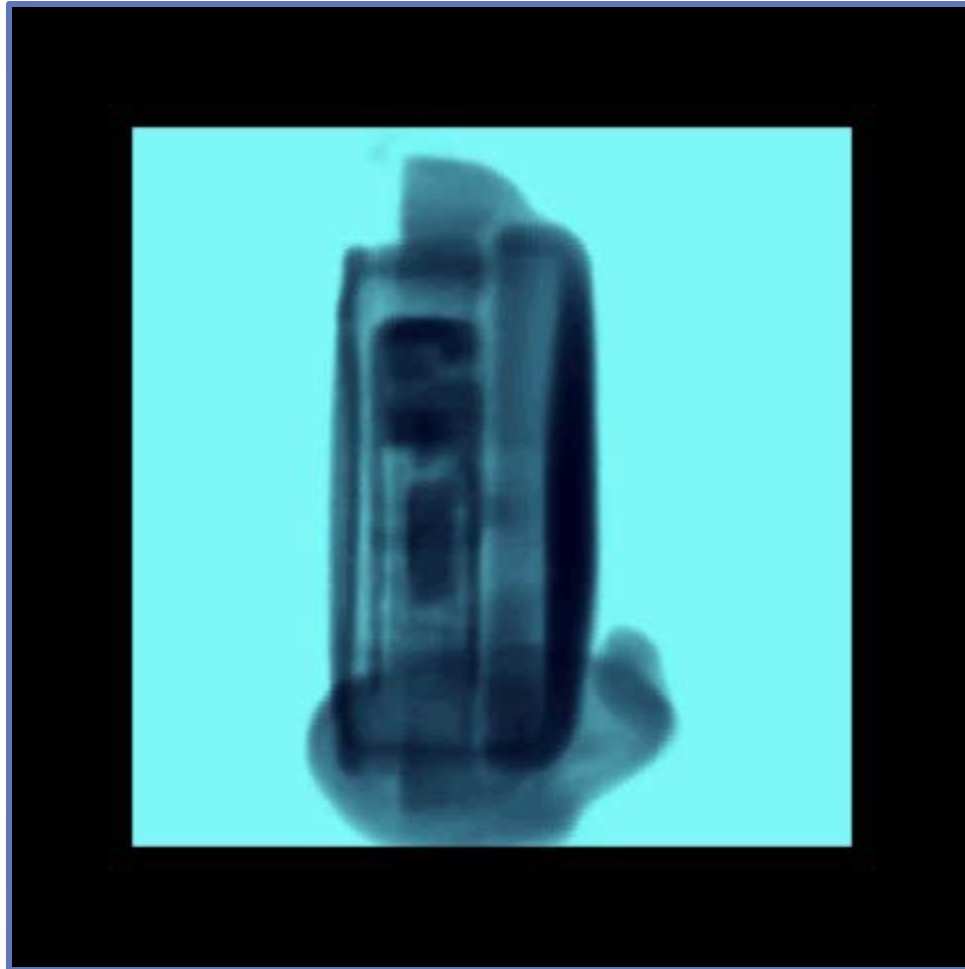
Contrast based neutron tomography

To obtain a tomography of a sample, a number of images must be collected at different angles, θ_i , ($0 \leq \theta_i < \pi/2$ or π) between sample and beam direction.

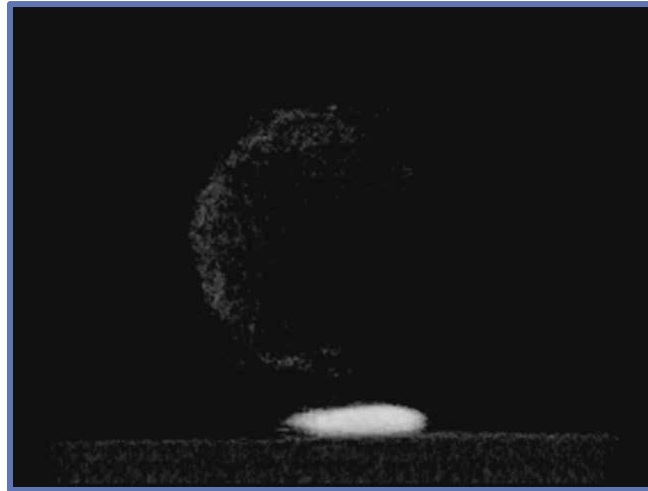


The sample is mounted onto a support which can rotate around an axis perpendicular to the beam and parallel to the scintillator plane.

A number of object projections is recorded over 180°

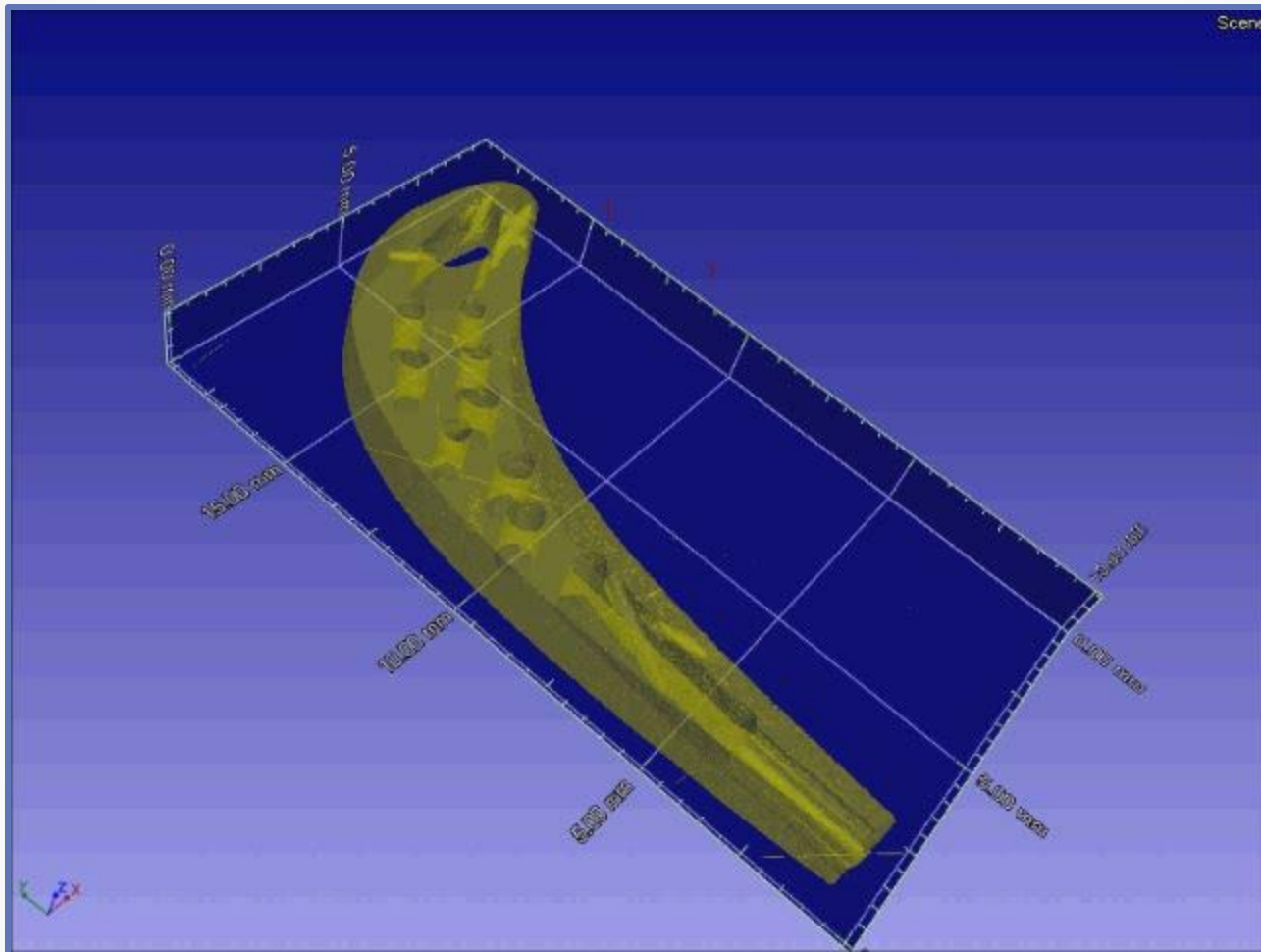


One of the many algorithms^[1] for tomography reconstruction can be applied to the collected images in order to obtain reconstructed slices without damaging the sample.



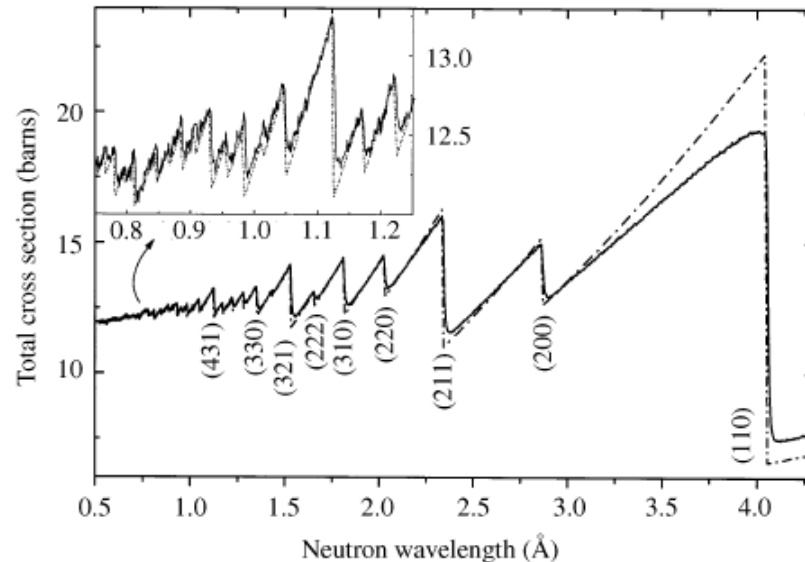
^[1] <http://www.slaney.org/pct/pct-toc.html>





Energy resolved neutron imaging

The transmission spectra of polycrystalline materials show sharp discontinuities as a result of coherent elastic scattering on the lattice planes.



Santisteban et al. *J. Appl. Cryst.* **34**, 289-297(2001)

These ***Bragg edges*** occur because, for a given hkl reflection, the Bragg angle increases as the wavelength increases until 2θ is equal to 180° .

At wavelengths greater than this critical value, no scattering by this particular $\{hkl\}$ family can occur and there is thus an increase in the transmitted intensity.

From Bragg's law, the wavelength at which this occurs is $\lambda = 2d_{hkl}$, giving a measure of the $\{hkl\}$ d -spacing in the direction of the incoming beam.

To exploit energy resolved imaging we need a monochromatic neutron beam.

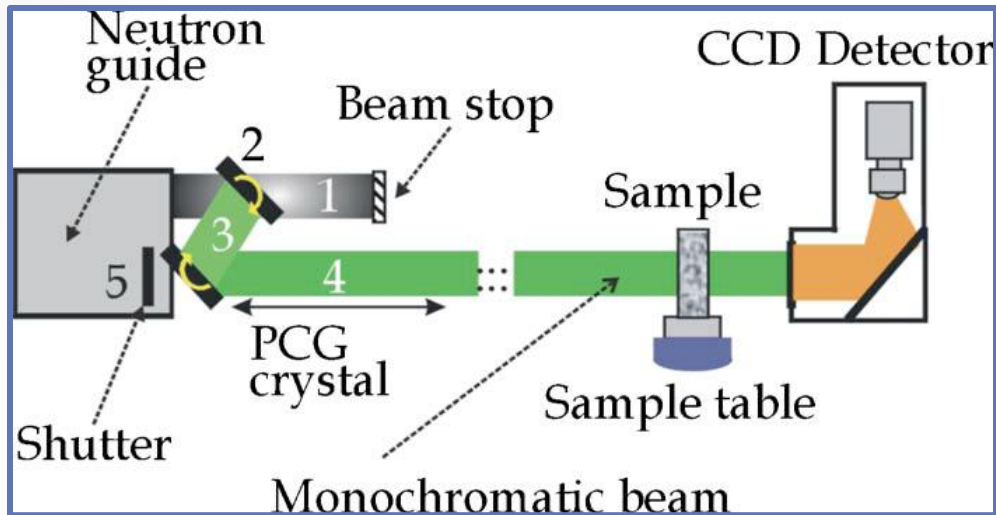
At continuous neutron sources, a neutron velocity selector can be used. It rotate at a constant angular frequency and have a spiral shape which only allows neutrons with the right speed to pass through.

By changing the rotational speed it is possible to change the wavelength

It is possible to obtain resolutions $\Delta\lambda/\lambda$ in the order of 10%



A special double monochromator system was tested at CONRAD in Berlin.



W. Treimer et al.
APPLIED PHYSICS LETTERS
89, 203504 (2006)

This construction enables to choose a monochromatic beam with a defined wavelength band $0.1 < \Delta\lambda/\lambda < 0.01$ between 2.0 and 6.5 Å.

The incoming neutron flux density is $\sim 2 \cdot 10^7 \text{ n} \cdot \text{cm}^{-2} \cdot \text{s}^{-1}$

The wavelength dependent output flux is $1 \cdot 10^5 \sim 2 \cdot 10^4 \text{ cm}^{-2} \text{ s}^{-1}$ enabling imaging with exposure times of 2–5 min/image.

At ***pulsed spallation*** sources, a linear accelerator produces bunches of energetic protons that are periodically made to collide with a heavy metal ***target***.

For each hit between a proton and a target atom, a number of neutrons (10 - 25) are produced.

After the interaction with the moderator nuclei, the neutrons leave the moderator with energies in the wanted energy range.

Because of the different energies with which they leave the moderator, neutrons with wavelength λ arrive at the detector with a time of flight (**TOF**), t , given by:

$$t = (m L / h) \lambda$$

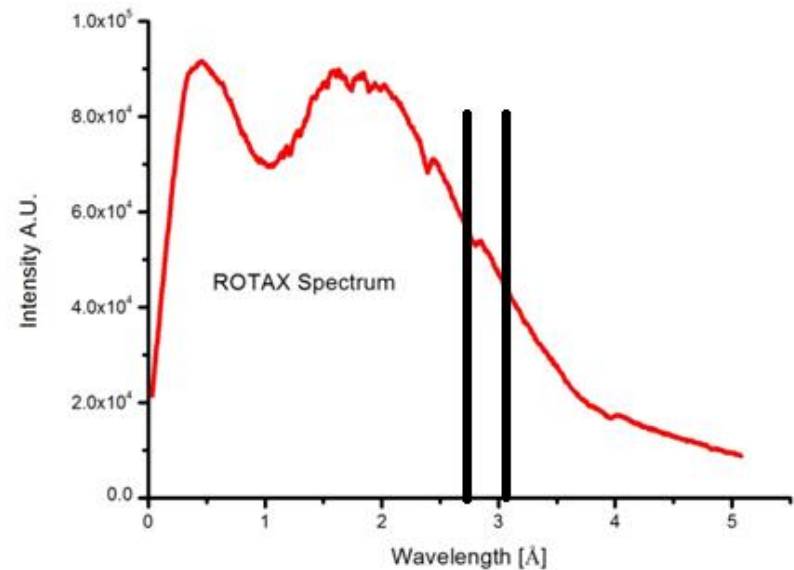
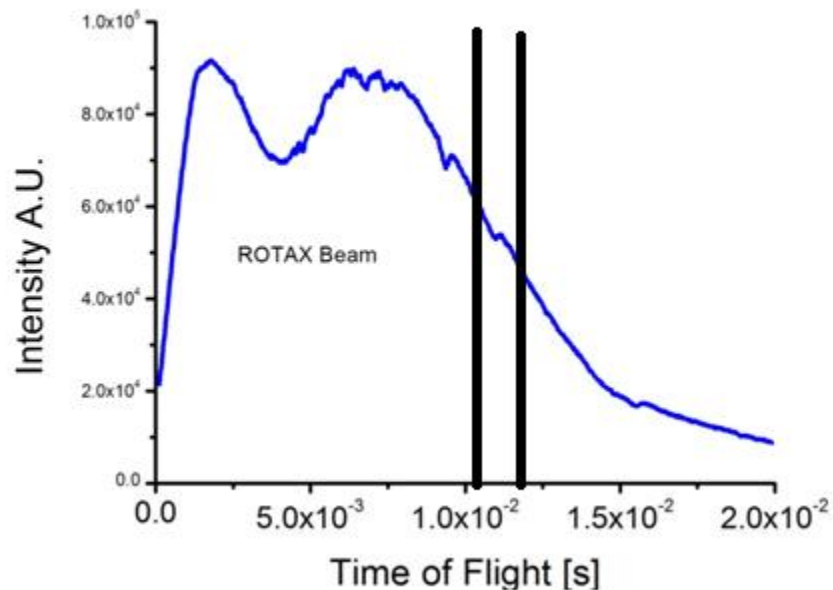
m is the neutron mass;

h is the Plank constant;

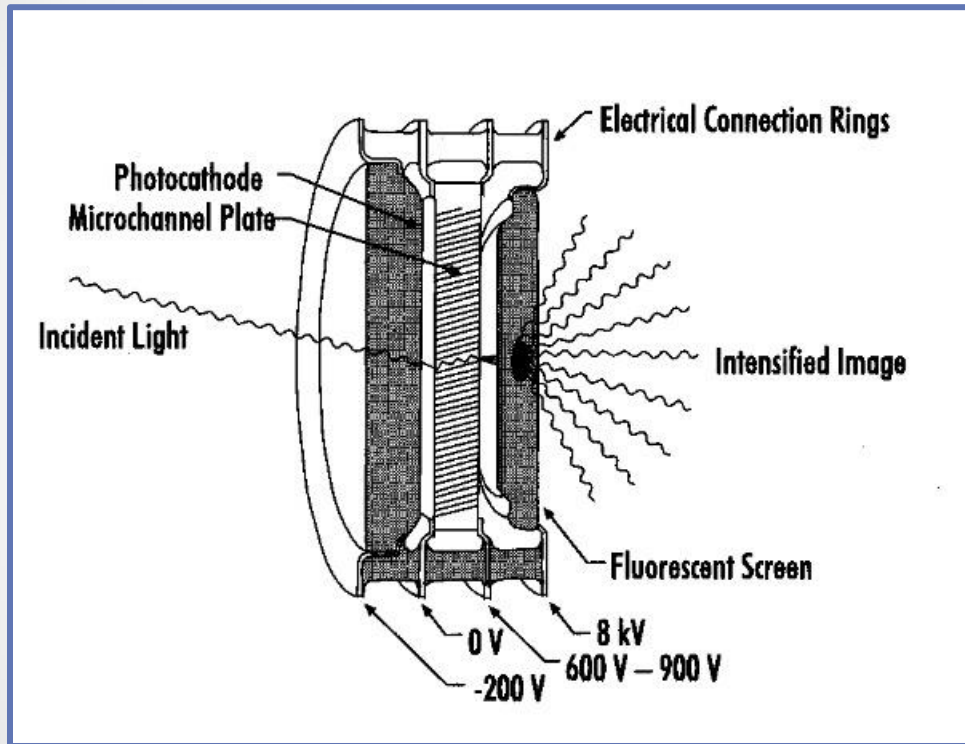
L is the flypath length.

By selecting neutrons in a well determined time relationship with the spallation pulse, we obtain a selection of neutron energies.

The two images below are the measured spectrum of the beamline ROTAX (ISIS - UK) in *TOF* (left) and *wavelength* (right).



Energy selection at pulsed sources can be easily obtained by an electronic shutter between the lens and the **CCD**.



Gated Image Intensifiers can allow very short optical gating times ($< 2\text{ns}$) so to reach any desired energy resolution.

Obviously, the greater the energy resolution, the lower the neutron flux.

There is a need for accumulating many partial images (one for each source pulse).

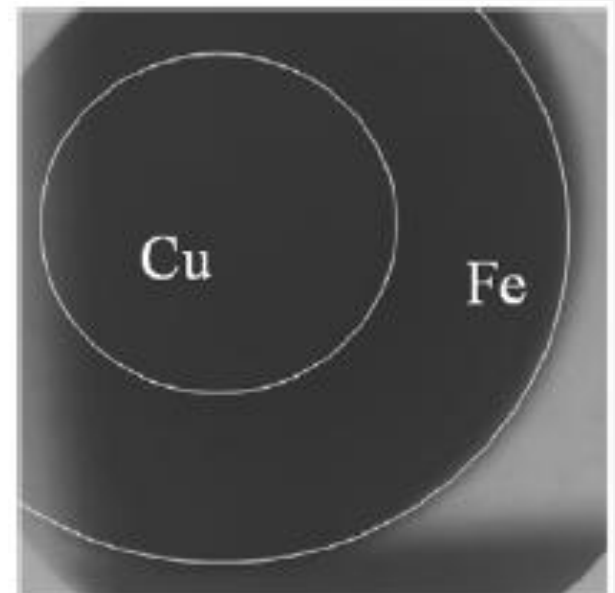
Recalling that the main source of noise in the **CCD** is the ***readout noise***, a technique called “***integrate on chip***” is used.

This avoids the continuous transfer of the partial images but, then, the thermal noise contribution can become determinant.

A deep cooling of the chip is mandatory.

Different materials may have similar absorbing values when integrated over the full energy range of the neutron beam.

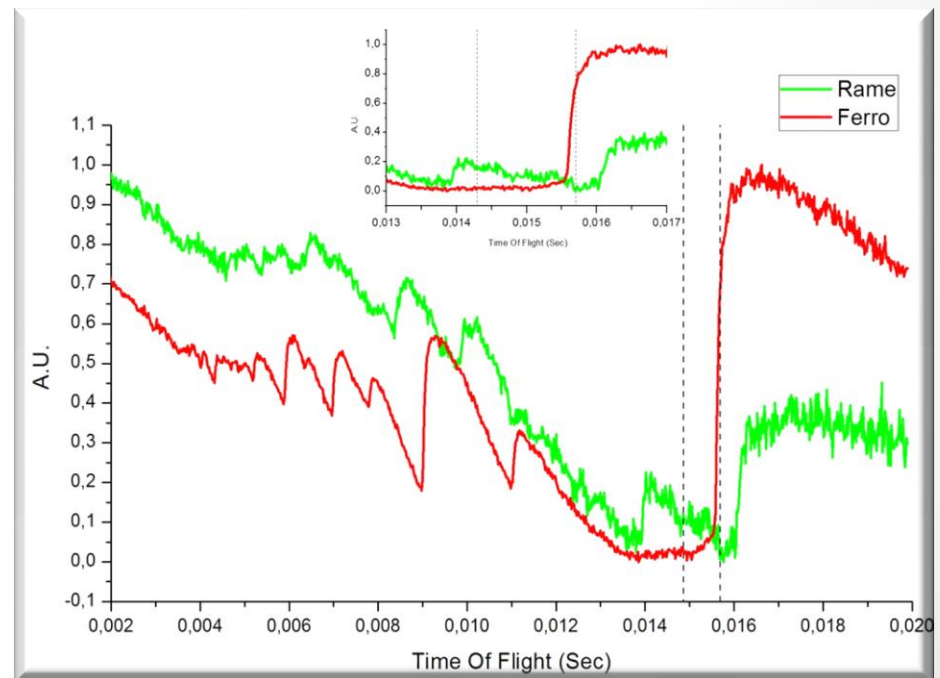
The two parts are almost impossible to differentiate in the full-beam neutron radiography.



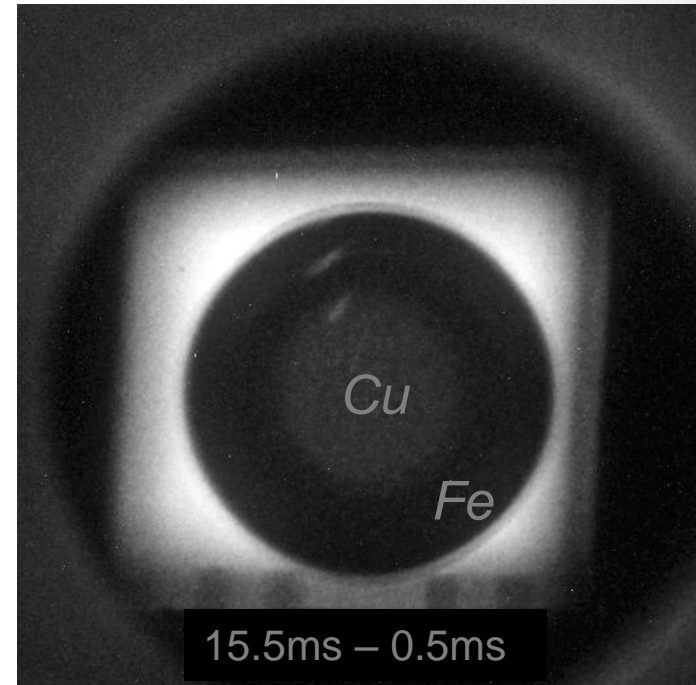
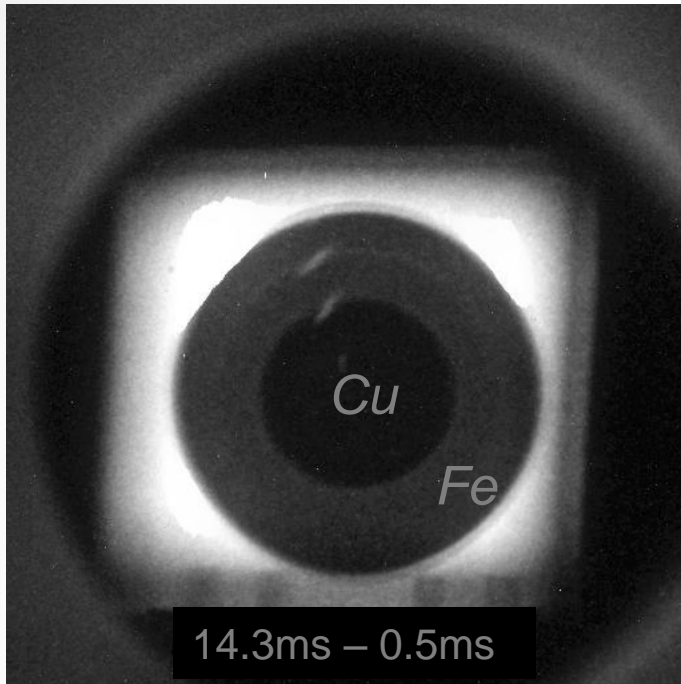
W. Kockelmann et al. Nuclear Instruments and Methods in Physics Research A 578 (2007)

Looking at the transmission spectra of the two materials it is possible to find energy values in which the transmission values are very different (because of the Bragg edges present in their transmission spectra).

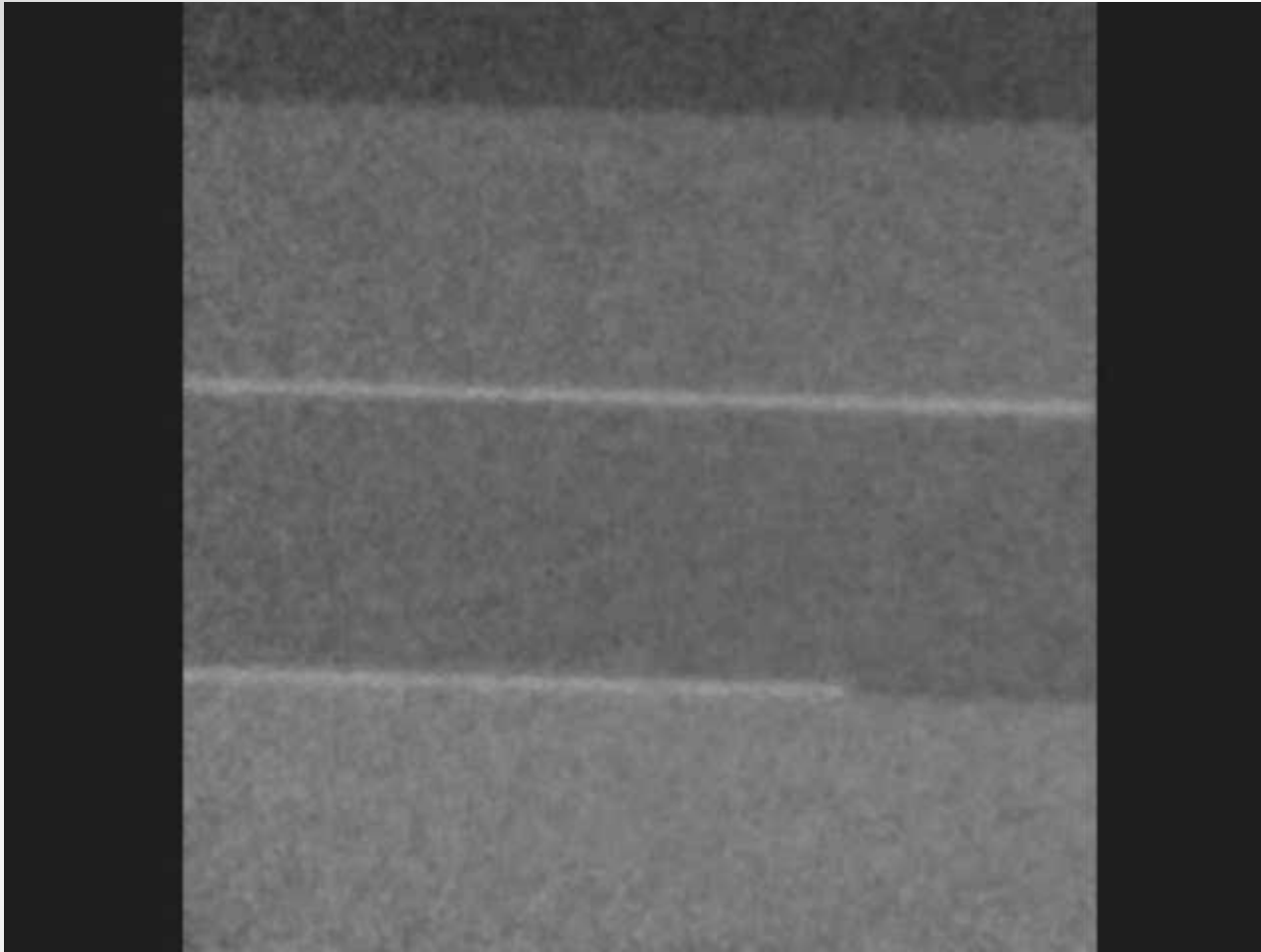
If we can take two radiography around that energy values, we can emphasize one or the other material.



V. Finocchiaro - Tesi di Laurea - Università di Messina (2010)



These images were acquired at the shown TOFs with multiple exposures of $500\mu\text{s}$ and summing many partial images for a ***total exposure time of 8s (400s of beam time @40Hz)***.

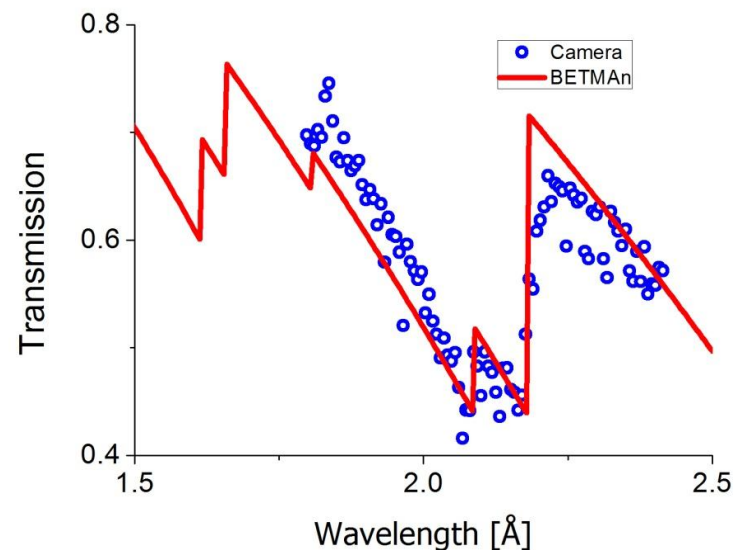
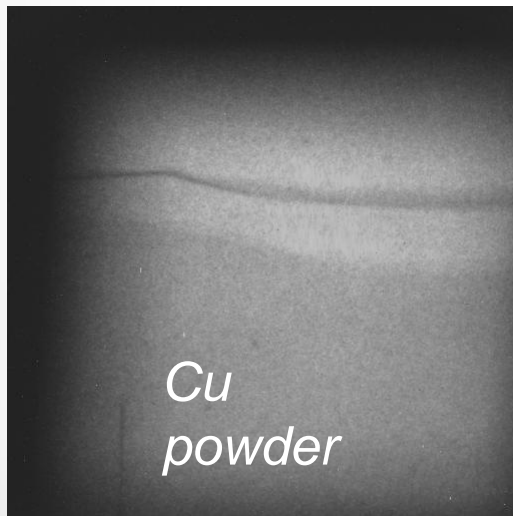


In this movie
three different
Cu crystals are
imaged at
different
wavelengths in
the range
1.8-4.3Å.

Each image is a sum of many images, each with an exposure time of **25μs**, for a **total exposure of 0.48s** (480s of beam time @40Hz).

This is one of a set of images of a **Cu** powder sample. The images were taken with **TOFs** in **7.0-9.4ms** range. (multiple exposure times of **25 μ s** for a total exposure time of **0.6s**, *i.e.* **600s of beam time @40Hz**).

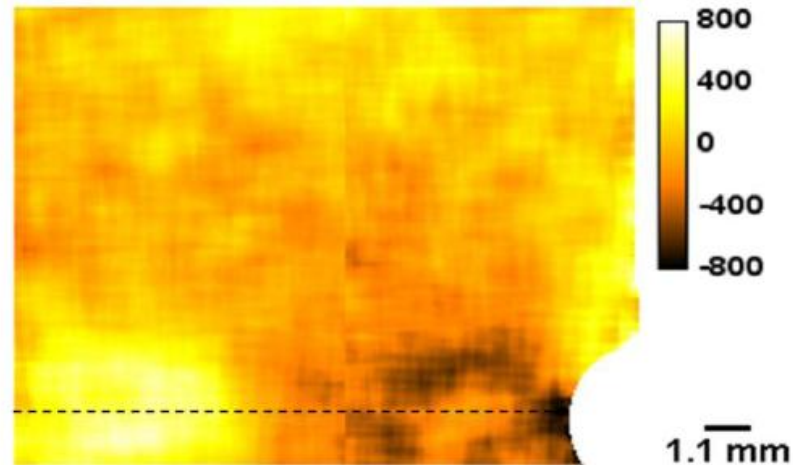
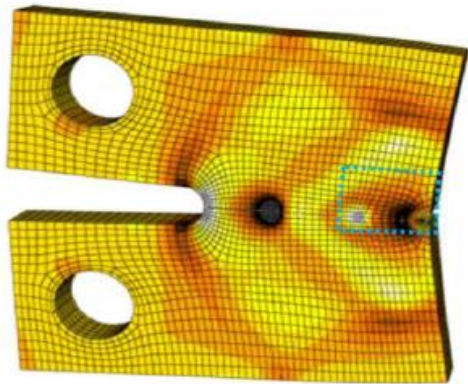
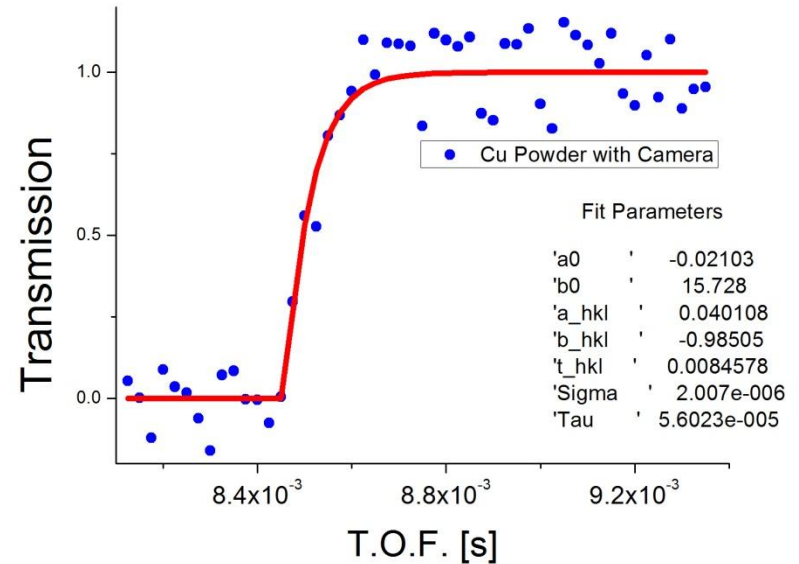
By plotting the transmission of a small region of the sample we can clearly see the **Bragg edges** due to the crystal planes.



*In principle, this information can be extracted for each pixel so as to have a spatial distribution of **d-spacings**.*

This can highlight the presence of strain or texture in a sample.

Model: See J.R.Santisteban et al.
Journal of Applied Crystallography vol.34 pp.289-297 (2001)



TOF technique for energy resolved imaging with CCD's based system has ***two major drawbacks***.

- timing characteristics of the $^6\text{LiF ZnS}$ scintillators
- ***the needed acquisition time***.

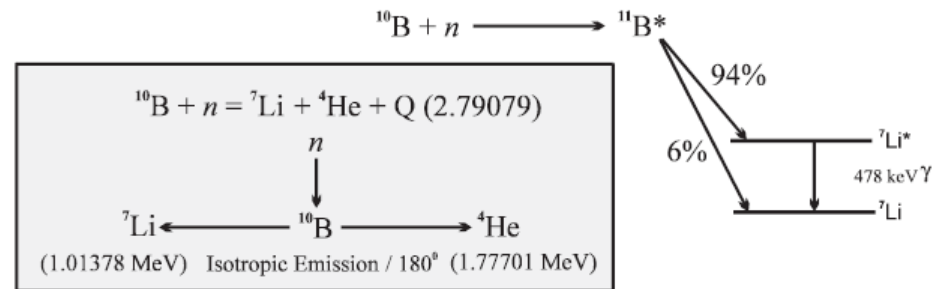
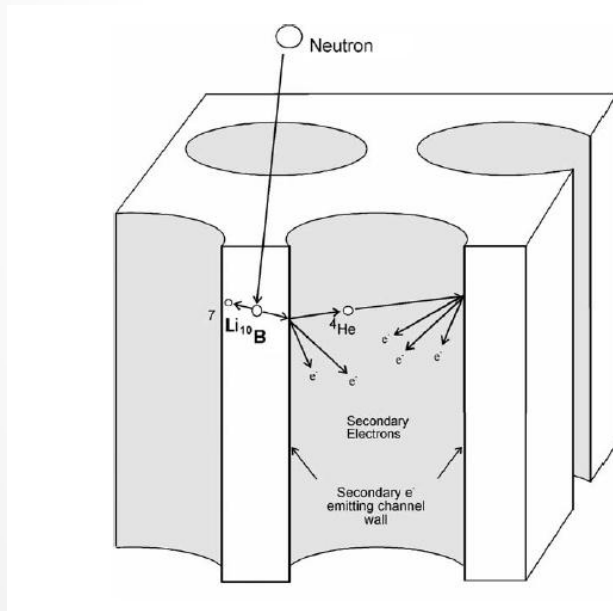
During the time interval (***~500s*** at ROTAX) needed to acquire an image, ***only a single wavelength band*** can be explored.

For a true strain analysis by neutron imaging we need a
different image detector !

A new image sensor that has been proposed as a more efficient, time resolved, image detector has been developed by *A. Tremsin* et coworkers and it is based on a ^{10}B -doped microchannel plate.

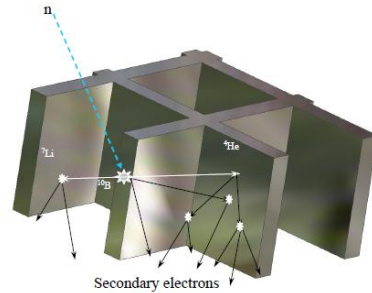


The neutron detection exploits the $^{10}\text{B}(n, \alpha) ^7\text{Li}$ reaction.

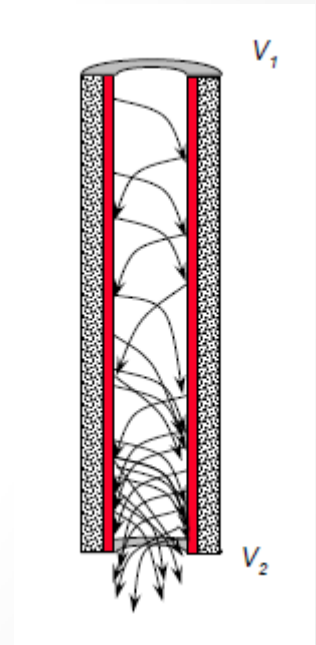


A.S. Tremsin et al. *Nucl. Instr. and Meth. A* **539** 278–311 (2005)

The *alpha* and ${}^7\text{Li}$ charged particle reaction products emerge from the channel wall surfaces into an open channel.



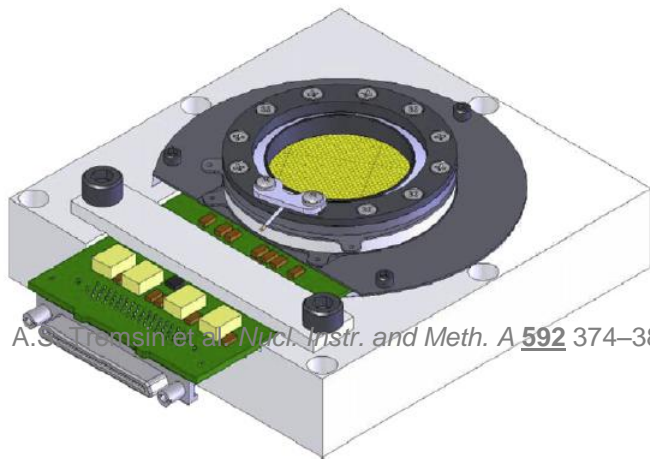
As these heavy particles cross the surface, a relatively large number of secondary electrons (and other species) are liberated to **generate a strong electron avalanche** and an output pulse.



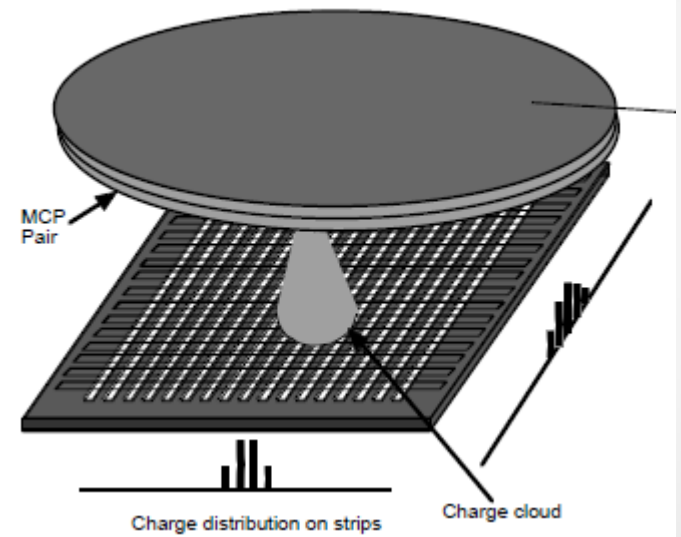
A.S. Tremsin et al. IEEE NSS 2007, October 2007

The neutron sensing **MCP** is combined with a fast readout device originally developed at CERN for high energy particles: **Medipix**.

Medipix is realized in CMOS technology and has a spatial resolution of $\sim 55\mu\text{m}$. It has 256×256 pixels and an active area of $14 \times 14 \text{mm}^2$.



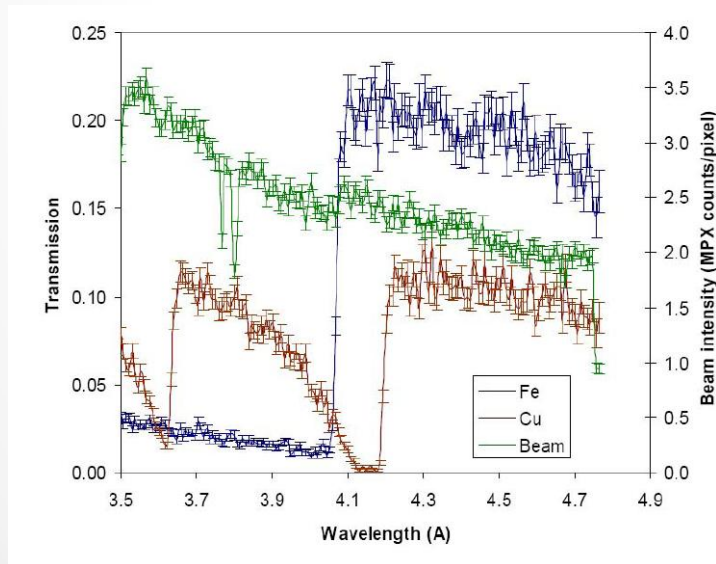
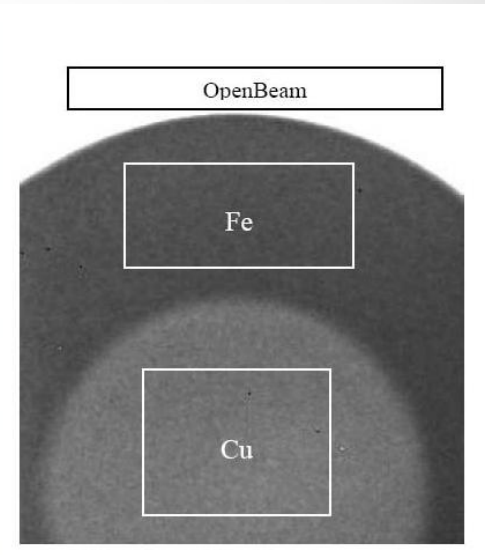
A.S. Tremsin et al. *Nucl. Instr. and Meth. A* **592** 374–384 (2008)



A.S. Tremsin et al. *IEEE NSS 2007*, October 2007

Energy-resolved radiography with the *MCP* detector on ENGIN-X.

Time width: 100 μ s.



Bragg edge spectra of the two metals compared to the open beam spectrum.

A.S. Tremsin Report on neutron transmission measurements at ISIS with a high resolution MCP detector (2008)

Delay = 0.003599



Imaging with polarized neutrons

N. Kardjilov et al. Nature Physics **4**, 399–403 (2008)

N.Kardjilov and coworkers developed an experimental method that combines *spin analysis* with *neutron imaging* and yields a new contrast mechanism for neutron radiography that allows for two- (images) and three-dimensional (tomography) investigations of magnetic fields in matter.

Neutrons are highly sensitive to magnetic fields due to their magnetic moment anti parallel to the internal angular momentum described by a spin **S** with the quantum number $s = 1/2$.

The fundamental idea of the method is to analyze the spin states in a beam after interaction with the sample for each pixel of an imaging detector and to determine spatially-resolved information about the spin rotation induced by the magnetic field of the sample.

The precession angle φ for a neutron traversing a magnetic field can be written as a path integral ^[1]

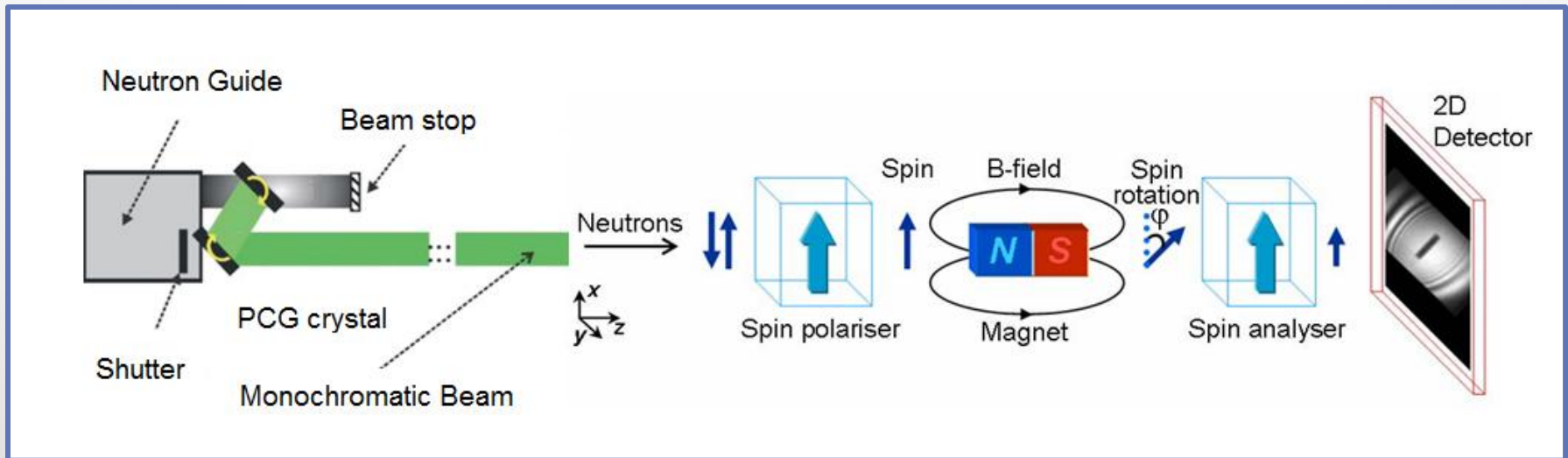
$$\varphi = \frac{\gamma_L}{v} \int_{path} B ds$$

Where:

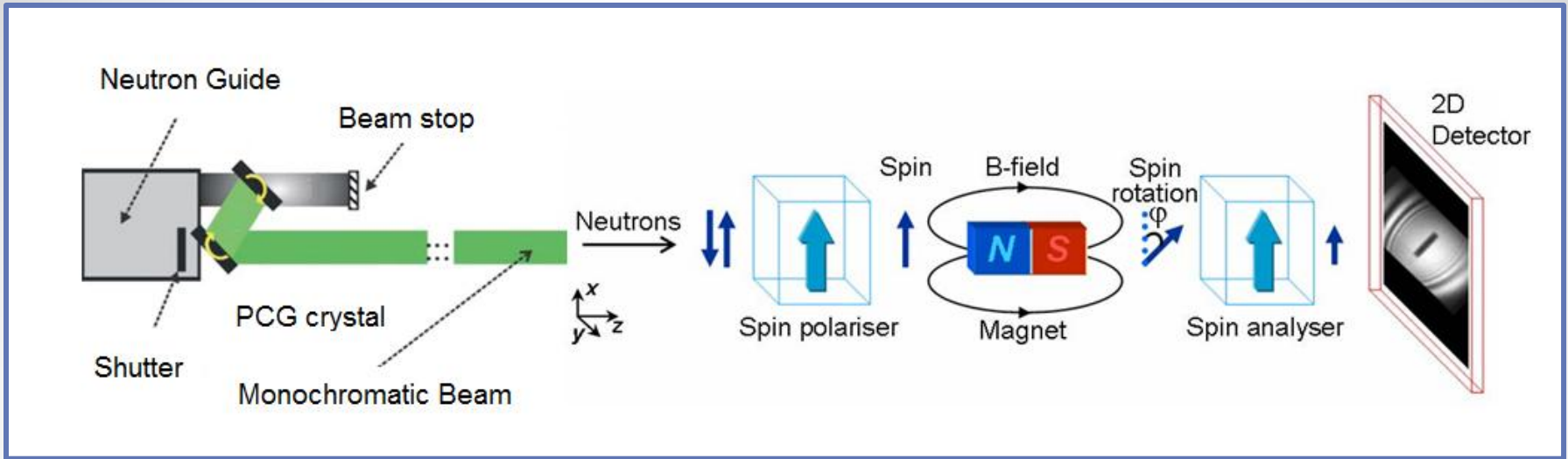
$\frac{\gamma_L}{v}$

is the gyromagnetic ratio of the neutron
is the velocity of the neutron

Since the spin precession in a magnetic field depends on the flight time in the field, the incident polarized beam has to be monochromatic (i.e. has to contain neutrons with a single velocity v).



[1] N. Kardjilov et al. Nature Physics **4**, 399–403 (2008)



The analyzer guarantees the passage of neutrons carrying a spin parallel to the initial polarization and absorbs neutrons with anti parallel spin.

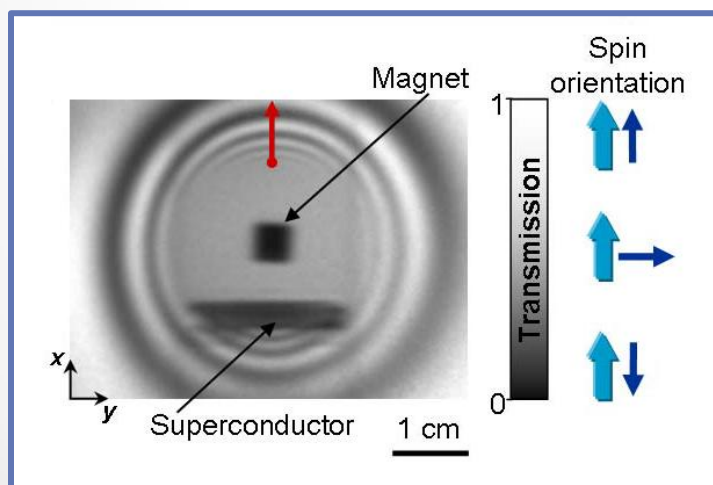
The detected image is superposition of conventional attenuation contrast, $I_a(x,y)$ and the contrast variations due to spin rotation $I_m(x,y)$:

$$I(x, y) = \underbrace{I_0(x, y) \cdot \exp\left(-\int_{\text{path}} \Sigma(s) ds\right)}_{I_a(x,y)} \cdot \underbrace{\frac{1}{2}(1 + \cos \varphi(x, y))}_{I_m(x,y)}$$

The cosine complicates the data interpretation with respect to the traversed magnetic fields.

But in many cases reverse approaches starting from an initial guess for the field distribution based on known symmetries, boundary conditions or reference values can be used for quantitative image analyses.

In some other cases three separate measurements with different polarization orientations are necessary.



Radiogram of a permanent magnet levitating over a $YBa_2Cu_3O_7$ superconductor.

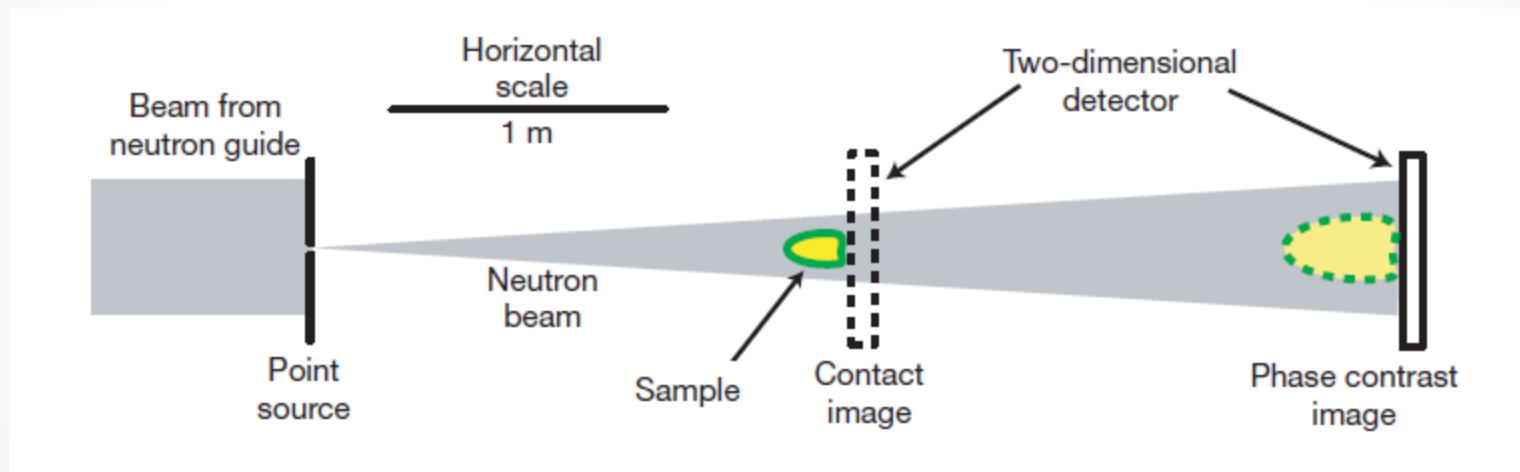
N. Kardjilov et al. Nature Physics **4**, 399–403 (2008)

Phase radiography with neutrons

B. E. Allman et al. Nature **408**, 158–159 (2000)

M. Strobl et al. Nucl.Instr. and Meth. B **266**, 181–186 (2008)

Propagation-based technique

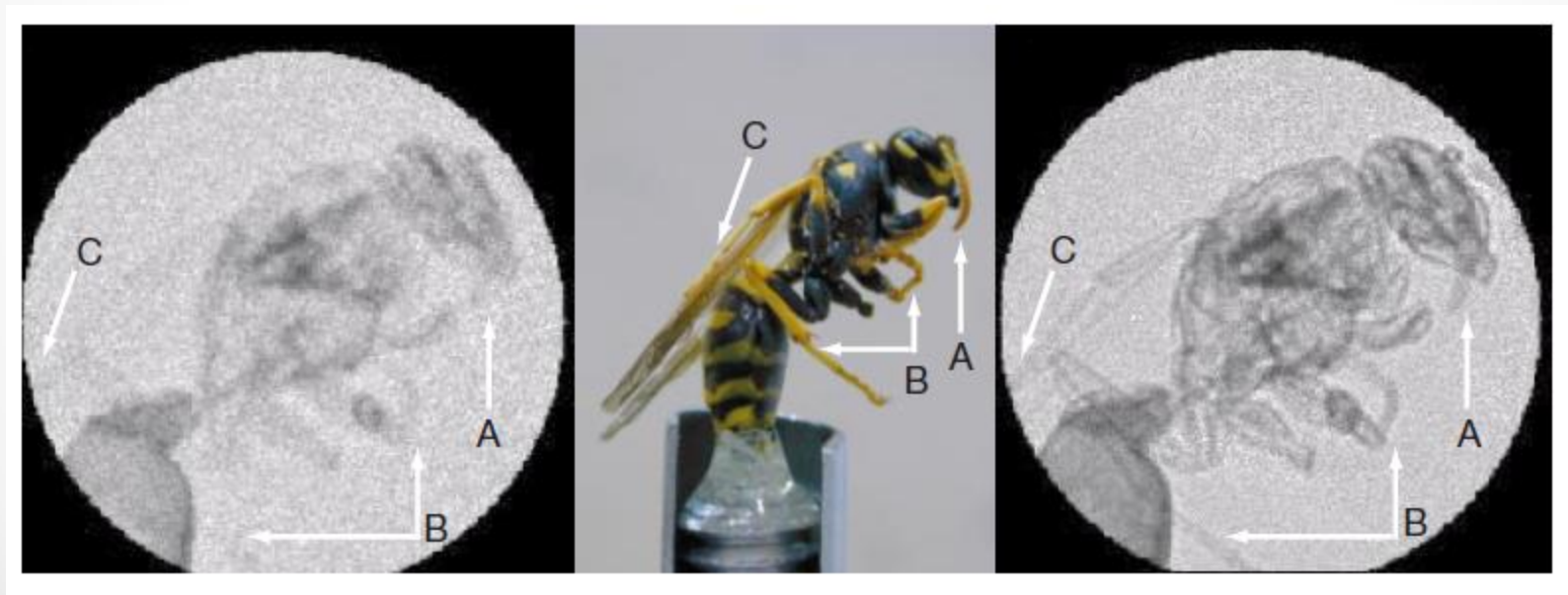


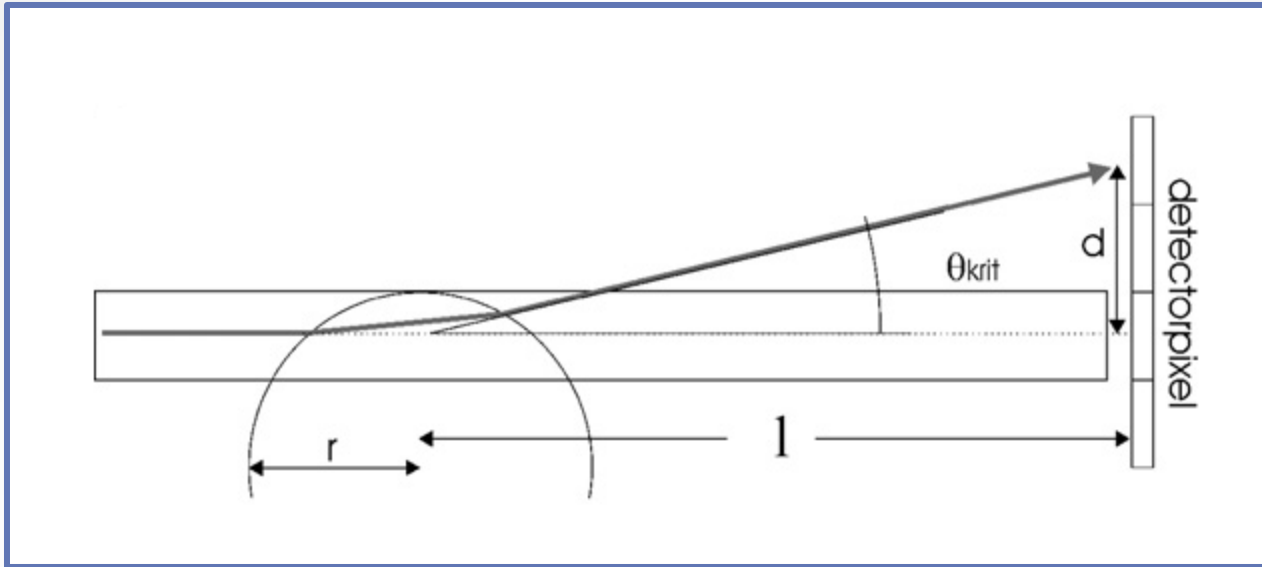
In a sample, not only the intensity of a beam, but also its phase changes due to the real part of the refractive index distribution, $\delta(x,y,z)$.

Phase gradients perpendicular to a beam induce deflections of the beam by angles

$$\alpha = \nabla_{\perp} \int_{path} \delta(s) \cdot ds$$

where $\delta = n-1$ is the real part of the refractive index





To induce refraction (phase) contrast, a refracted beam would have to gain a spatial deviation (from the incident ray) of at least 2 pixel at the detector position.

Recalling the relation that defines the spatial resolution, we need to reduce the source dimension, D , in order to maintain a good spatial resolution despite the increased ℓ value.

$$d = \ell \frac{D}{L} = \frac{\ell}{L/D}$$

*Thank you
for
your attention*